Resistance and heteroresistance as a consequence of colistin therapy during *Acinetobacter baumannii* murine pneumonia

Running title: Evolution of colistin resistance in mouse infection model

Juan Hernandez-Bird[1]; Bixi He[1]; Leah M. VanOtterloo[2]; Elizabeth B. Billings[1]; Wenwen Huo[1]; Gabriella I C Teodoro[1]; Haley Echlin[3]; Jason M. Rosch[3]; M. Stephen Trent[2]; Ralph R. Isberg[1*]

[1] Department of Molecular Biology and Microbiology, Tufts University School of Medicine, MA, USA

[2]Department of Microbiology, College of Arts and Sciences, University of Georgia, GA, USA

[3]Department of Infectious Diseases, St Jude Children's Research Hospital, TN, USA

*Corresponding author contact: ralph.isberg@tufts.edu

Abstract:

Acinetobacter baumannii is an ESKAPE pathogen linked to healthcare-associated diseases. Due to evolved resistance, last-resort antibiotics such as the lipooligosaccharide (LOS)-targeting colistin are increasingly used to treat multidrug-resistant isolates. To track the evolution of colistin resistance within a host, we performed sequential oropharyngeal infections in immunocompetent or immune-depleted mice in the presence of inhaled colistin. Both resistant and heteroresistant *A. baumannii* strains emerged with *pmrB* mutations that efficiently competed with the susceptible parent in the presence of colistin. The *pmrB* mutants had a fitness cost in immunocompetent mice in the absence of colistin treatment but retained their ability to colonize the host. In contrast, LOS-deficient *A. baumannii* mutants removed the target of colistin, but such mutants were unable to colonize the lung. The two pathogenic *pmrB* mutants showed clear evidence of LOS modification, which was linked to increased transcription of LOS modification enzymes, including the product of the cryptic *eptA* gene. Spontaneous insertion mutations that caused hyperexpression of *eptA* allowed the heteroresistant mutant to develop clinically-significant colistin resistance. Insertion mutations upstream of the *eptA* gene or those disrupting *hns*, which encodes a small histone-like protein, resulted in increased *eptA* transcript, linking expression of this protein to clinically significant resistance. The resistant variant selected from the heteroresistant parent was stable in the absence of drug, but continued passaging selected for colistin-resensitized pseudorevertants that were largely due to disruption of the LOS modification enzymes. Therefore, colistin heteroresistance is an early stage in the stepwise acquisition of stable resistance in *A. baumannii*.

Significance:

The mutational pathways leading to antibiotic-resistant infections and the role of the immune system in preventing them are poorly understood. Here we employed a colistin-treated mouse pneumonia model of *Acinetobacter baumannii* and observed the evolution of colistin-resistant and heteroresistant mutants in immune-depleted and immunocompetent hosts, respectively. We show that mutations that result in alteration of colistin's target drive evolutionary pathways to resistance, whereas removal of the target is unlikely to be clinically significant. We demonstrated that the heteroresistant mutant generates subpopulations with higher levels of resistance through insertion mutations in specific gene regions. This study furthers our understanding of how resistance emerges during infection and provides a genetic explanation for the transition from colistin heteroresistance to full resistance.

Introduction:

Antibiotic-resistant infections caused by the ESKAPE group of pathogens are an urgent global health concern, with lethality predicted to surpass cancer by 2050(1). Belonging to this group is *Acinetobacter baumannii*, a Gram-negative bacterium with a remarkable ability to evolve resistance to currently employed antibiotics(2). As an opportunistic pathogen, *A. baumannii* mainly affects wounded or immunocompromised patients in healthcare settings with respiratory, bloodstream and urinary tract infections being its most concerning clinical manifestations(3, 4). The World Health Organization currently classifies carbapenem-resistant *A. baumannii* in the highest priority category for research and development of treatment options(5). Therefore, understanding how this organism evolves to give rise to drug-resistant variants is of the upmost importance.

Resistance to the first-line antimicrobial carbapenems is increasingly common in *A. baumannii* clinical isolates(6), so last-resort antibiotics are currently being employed against extensively drug-resistant *A. baumannii*(7). Colistin is one such antimicrobial, but its usefulness is limited due to concerns about its nephrotoxicity. New inhalation therapies are being pursued for the treatment of respiratory infections in hopes of reducing toxic side effects(8, 9). The drug is a positively charged peptide that binds to the negatively charged phosphate groups on the lipid A component of lipopolysaccharide (LPS), or lipooligosaccharide (LOS) in the case of *A. baumannii,* leading to envelope disruption and cell lysis(7).

Gram-negative bacteria have evolved multiple strategies to modify the lipid A component of LPS/LOS to increase resistance to antimicrobial peptides(10). In *A. baumannii,* colistin resistance is mainly caused by mutations within the *pmrCAB* operon(11). The PmrAB cassette is a two-component system that responds to low pH and select divalent cations (Fe^{2+}, Zn^{2+}, Al^{3+}), controlling the expression of multiple genes including *pmrC* and the *naxD* operon(12). *pmrC,* also known as *eptA*, encodes a phosphoethanolamine transferase that adds phosphoethanolamine to the 1- and 4' phosphoryl groups in lipid A(13). *naxD* encodes a YdjC family deacetylase that plays a part in the addition of galactosamine to the 1- phosphoryl group in lipid A(14). These modifications reduce both the negative charge and LOS affinity for polymyxins such as colistin(13). Mutations in *pmrAB* genes can lead to the constitutive activation of this system by the PmrA positive regulator, resulting in polymyxin resistance. In addition, some strains of *Acinetobacter* possess an orphan homologue of the PmrC/EptA phosphoethanolamine transferase, that is also under the control of PmrAB. For simplicity, we will refer to the orphan copy as *eptA* and the *pmrAB*-linked copy as *pmrC.* Clinical isolates with high colistin resistance

have been characterized that overexpress *eptA* transcript as a consequence of insertion sequence transposition into regions upstream of *eptA*(15, 16).

Mutations in *pmrAB* have also been linked to colistin heteroresistance in *A. baumannii*(17). Antibiotic heteroresistant strains generate subpopulations resistant to the exposed antibiotic at much higher frequencies than observed for sensitive strains(18). Heteroresistant pathogens are troubling because current clinical microbiology methods frequently classify them as susceptible, and their genetic background could provide an intermediate step towards the evolution of traditional resistance(19–21). The genetic mechanisms facilitating this phenomenon are poorly understood, but recent evidence points to transient gene amplification in the resistant subpopulation, which occurs at a higher frequency than observed for spontaneous mutations(22). Amplification and mutations in genes that regulate or mediate the modification of lipid A have been reported to contribute to colistin heteroresistance in pathogens other than *Acinetobacter*(23–26). The genetic basis for colistin heteroresistance in *A. baumannii*, however, appears unrelated to amplification.

A. baumannii is one of the few known species with the ability to survive with an LOS-deficient outer membrane(27). LOS-deficient mutants are readily isolated in a subset of clinical isolates during *in-vitro* experimental evolution to polymyxins but are rarely reported in clinical studies(28). Absence of LOS, usually due to mutations in the early LOS biosynthesis genes, results in high-level colistin resistance but is accompanied by outer membrane instability and a high fitness cost(29). Nevertheless, these LOS-deficient mutants may provide transition states to more virulent, drug-resistant mutants(30, 31). Inactivation of PBP1A glycosyltransferase activity allows viability in the presence of LOS knockout mutations(32). Additionally, mutations in the *pldA* and *mla* genes, enzymes that act to reduce glycerophospholipid content in the outer

membrane, alleviate the severe growth defect in LOS-deficient strains(27). It is unknown if these suppressor mutations allow LOS-deficient strains to retain their virulence.

Previously, we performed serial passaging of the low virulence *A. baumannii* ATCC17978 strain in a murine pneumonia model during treatment with ciprofloxacin(33). In immune-depleted animals, drug-tolerant/persistent mutants arose that resulted in antibiotic treatment failure and the emergence of second-step drug-resistant mutants. Neither class of mutants achieved high population levels in the lines passaged in immunocompetent hosts(33, 34). More recent multi-drug resistant *A. baumannii* clinical isolates have been proposed as more relevant for infection modeling due to their ability to cause lethal pneumonia even in the absence of immune depletion(35). One of these strains is *A. baumannii* LAC-4, a multi-drug resistant specimen that was isolated from a Los Angeles County outbreak in 1997(36–38). In this study, we performed experimental evolution in this highly mouse-virulent strain, identifying multiple routes to colistin-resistant virulent isolates, as well as forbidden routes that result in avirulent strains.

Results:

Sequential lung infections in the presence of nebulized colistin select for pmrB mutations.

To better simulate the conditions in which *A. baumannii* evolves colistin resistance, we performed 16 sequential lung infections with the LAC-4 strain in both immune-depleted and immunocompetent mice treated with inhaled colistin (Fig. 1A). Immune-depleted animals received two intraperitoneal injections of cyclophosphamide, a chemotherapeutic agent that

induces profound neutropenia and significantly reduces lymphocyte and monocyte counts(39, 40). Lung infections were established via oropharyngeal inoculation in both sets of animals. Three separate lines were maintained per condition, and lung bacterial burden after 24-hour infections was quantified (Figs. 1B, C). The inoculum CFU for the immune-depleted lines was reduced in the second and fifth passage to ensure effective antibiotic selection throughout the experiment (2×10^2 CFU below the expected bacterial burden; Fig. 1B). Line A showed evidence of antibiotic treatment failure after 13 passages in the immune-depleted animals, with bacterial burdens approaching that observed in untreated animals. In contrast, colistin treatment consistently reduced bacterial burden in the other two immune-depleted lines and in the immunocompetent lines throughout all passages (Figs. 1B, C).

Colistin-resistant *A. baumannii* isolates are defined by the Clinical Laboratory Standards Institute (CLSI) as being able to grow at colistin concentrations $\geq$ 4μg/mL(41). The parental LAC-4 strain is colistin-susceptible, so saved pools were plated on LB agar supplemented with 0-4μg/mL colistin to detect the presence and abundance of colistin-resistant isolates (Figs. 1D, E and Fig. S1). During passaging in the immune-depleted animals, colistin-resistant colonies emerged in all three lines, but only in line A did the proportion of resistant clones increase and overgrow the susceptible ancestor (Fig. 1D). Whole genome sequencing (WGS) of saved resistant isolates from line A revealed they all have the *pmrB(*T235I) mutation that has been previously described in polymyxin-resistant *A. baumannii* strains(42).

Colistin-resistant colonies emerged in lines B and C in the last three passages through immunocompetent animals (Fig. 1E). WGS of resistant isolates in line C revealed that they all possessed the *pmrB*(A236E) mutation that had been associated previously with polymyxin resistance(43). Due to their increase in proportion on solid medium containing 4μg/ml colistin on

successive passages through mice, the *pmrB*(T235I) and *pmrB*(A236E) clones were selected for further characterization. Importantly, the *pmrB*(T235I) strain employed in this study contains three additional IS*Aba* insertion mutations discussed later on. In addition, other mutants were isolated at low colistin concentrations, subjected to MIC determination and WGS, but they were not studied further (Fig. S1 and Dataset S1). Thus, colistin treatment in both immune host states selected for *A. baumannii* isolates with mutations in the region encoding the PmrB histidine kinase domain during passage in the experimental pneumonia model.

The fitness cost of the LAC-4 pmrB mutants.

Mutations that promote antibiotic resistance are often associated with fitness costs(44, 45). The continuous spread of drug-resistant bacteria requires that resistant mutants compete efficiently with fully virulent parental organisms in mammalian tissues(46). Therefore, we tested the hypothesis that mutations selected during lung infections would confer resistance without compromising the ability of the LAC-4 to colonize the host, and would compete efficiently with the parent in the presence of colistin.

The two evolved *pmrB* mutants were compared to WT LAC-4 during growth in broth culture. The *pmrB*(T235I) mutant, which had been selected in the immune-depleted animal, had a significant increase in broth doubling time compared to its LAC-4 parent (Fig. 2A; $p \leq 0.05$). In contrast, the *pmrB*(A236E) mutant that was selected in the immunocompetent animal showed no significant change in doubling time during broth growth (Fig. 2A). To determine the relative fitness of the evolved *pmrB* mutants compared to WT during lung infection, strains were mixed 1:1 (mutant:WT) and competition experiments were performed during experimental lung infections in the presence or absence of immune depletion (Figs. 2B, C). In the absence of colistin treatment, the evolved *pmrB* mutants exhibited a competition deficiency against WT in

the immunocompetent host, with the *pmrB*(T235I) mutant exhibiting the larger defect (Fig. 2B). In contrast, there was no significant competition defect against WT when the competition was performed in immune-depleted hosts (Fig. 2C). The gentamycin-susceptible LAC-4 strain (*ΔpABLAC2*) was included in this study since it exhibits no significant change in colistin sensitivity and growth rate *in-vitro*, allowing us to perform WT vs WT mouse competitions as a control (Figs. 2A-C). These results demonstrate that in the absence of colistin, *A. baumannii pmrB* mutants experimentally evolved during lung infections can be negatively selected in the presence of an intact immune response.

To reconstruct the fitness advantage of *pmrB* mutants relative to the parental control in the presence of colistin, each mutant was mixed with WT at 5:95 ratio and passaged through either immune-depleted or immunocompetent mice treated with colistin (Figs. 2D, E). After only two successive passages in the lung, the *pmrB*(T235I) mutant lines reached 100% of the total population in the immune-depleted host (Fig. 2E). Notably, during colistin treatment, this mutant also reached a high proportion of the population (>85%) in all lines after three passages in the immunocompetent host (Fig. 2D), even though this mutant competed poorly with wild type in the absence of drug pressure (Fig. 2B). The *pmrB*(A236E) mutant also showed evidence for effective competition during passaging in both host conditions, but constituted smaller proportions of the populations than that observed for the *pmrB*(T235I) mutant, with competitions not uniform among all the lines (compare Figs. 2D and 2E). Therefore, the *pmrB*(T235I) mutant selected in the immune-depleted conditions established a colistin-resistant population more efficiently than the *pmrB*(A236E) strain, even in the presence of an intact immune response.

Colistin-resistant LOS-deficient strains show poor fitness during murine pneumonia.

As the colistin-resistant mutations identified in the murine pneumonia model resulted in altered regulation of the PmrAB control system but did not directly disrupt LOS biosynthesis (Fig. 3A), we asked whether LOS biosynthesis dysfunction was an available mutational pathway to achieve colistin resistance during LAC-4 infection. A subset of *A. baumannii* clinical isolates can acquire resistance to polymyxins through mutations causing defective LOS biosynthesis ($LOS^{(-)}$)(28). To determine whether the parental LAC-4 strain could tolerate $LOS^{(-)}$ mutations, we first selected for colistin-resistant LAC-4 isolates and then screened for collateral vancomycin sensitivity (Fig. 3B). $LOS^{(-)}$ mutants have a compromised outer membrane resulting in susceptibility to antibiotics usually ineffective against Gram-negative bacteria(27). We identified one such isolate and whole genome sequencing revealed a single *lpxA* G142R (*lpxA**) mutation, predicted to disrupt LOS synthesis (Dataset S2). SDS-polyacrylamide gel analysis of protease-treated extracts showed that, in contrast to the *pmrB* mutants, the *lpxA**-containing strain showed no evidence of LOS comigrating with the parental LAC-4 WT strain (Fig. 3A).

Due to low fitness, $LOS^{(-)}$ strains revert to $LOS^{(+)}$ or acquire second-site mutations that alter the glycerophospholipid composition of the outer membrane(27, 28, 32, 47). $LOS^{(-)}$ suppressor mutants were selected by growing the LAC-4 *lpxA** mutant on LB solid medium at 42°C, a temperature that exacerbates its growth defect and results in a fine lawn of growth (Fig 3B). After selection, 16 non-reverted colonies that grew above the lawn were saved and subjected to WGS. Mutations identified in this fashion included a frameshift in *pldA*, as well as missense mutations in the *ponA* gene, both of which had been previously identified as increasing the growth rate of $LOS^{(-)}$ strains (Dataset S2) (27, 32). A quadruple mutant containing a mutation in *msbA*, a gene involved in lipooligosaccharide transport across the membrane, was also

isolated(48). Additionally, *pldA* mutants with second step mutations in ABLAC_25350, which encodes a hypothetical protein, were also isolated but were not studied further (Dataset 2).

Three non-identical LOS$^{(-)}$ suppressor mutants were chosen for further analysis, each of which had either a *pldA* mutation or *pldA ponA* mutations (Fig. 3B). The three suppressor mutations showed no evidence of the reversion to LOS production, as the LOS profile of proteolyzed samples fractionated on SDS gels were indistinguishable from the *lpxA** mutant (Fig. 3A). Furthermore, analysis by thin layer chromatography (TLC) showed that these suppressor mutants remained LOS deficient (Fig. 4C). Growth rates in LB were determined for each of the LOS$^{(-)}$ strains. The *lpxA** mutant had a drastic increase in doubling time (38mins) compared to its WT parent (22mins) (compare Figs. 2A and 3C). All three LOS deficient suppressor mutants exhibited significant improvements in doubling time (32-35mins; Fig. 3C). Therefore LAC-4 tolerates LOS deficiency, and similarly to other *A. baumannii* strains, mutations in the *pldA* and *ponA* genes enhance fitness.

Although readily selected *in-vitro,* LOS$^{(-)}$ clinical isolates have rarely, if ever, been observed and none emerged during passaging(49). Few studies have tested the virulence of LOS$^{(-)}$ *Acinetobacter baumannii* mutants(50–52), and none, to our knowledge have tested the impact of suppressor mutations on its pathogenesis. To determine their relative defects during murine pneumonia, the LOS$^{(-)}$ strains were mixed at a 1:1 ratio with WT, inoculated into either immune-depleted or immunocompetent mice, and competitive indices were determined (Figs. 3D, E). In both host states, all LOS$^{(-)}$ mutants had a devastating competition defect relative to WT, varying from 10^{-4} – 10^{-5} compared to the initial inoculum (Figs. 3D, E). This colonization efficiency was more than 1000X lower than observed for the *pmrB* mutants that had been selected during lung infection (compare Figs. 3D, E vs Figs. 2B, C). The suppressor mutations

showed a fractional increase in the competitiveness relative to the parental *lpxA** strain when competitions were performed specifically in immunocompetent animals, with *lpxA** *pldA** *ponA** showing a significant increase in competitiveness (Fig. 3D). Even so, these suppressor mutations fail to compensate for the drastic colonization defects exhibited by LOS$^{(-)}$ strains.

Paths to colistin resistance occur via LOS modification and elimination.

To both confirm and quantify the level of colistin resistance in our evolved strains, colistin E-test strip analysis was performed (Fig. 4A). All LOS$^{(-)}$ strains surpassed the breakpoint for clinical resistance (≥4μg/mL) with the suppressor mutants showing colistin minimum inhibitory concentration (MIC) values that were higher than the *lpxA** parent (Fig. 4A). The WT LAC-4 strain was confirmed to be colistin susceptible and the *pmrB*(T235I) mutant was highly colistin-resistant based on MIC determination (Fig. 4A). Surprisingly, the *pmrB*(A236E) mutant only had a slight increase in colistin MIC compared to WT based on the E-test determination and was clearly still susceptible based on the clinical drug resistance breakpoint definition (Fig. 4A).

As mutations in *pmrB* appear to be preferentially selected during disease because of their relatively high fitness compared to those lacking LOS(50–52), the genetic and biochemical basis of the two *pmrB* alleles was pursued. Similar to our observations modeling disease during mouse passage, colistin-resistant *Acinetobacter baumannii* clinical isolates primarily have mutations in *pmrB*(53). PmrB is the sensor kinase of the PmrAB two-component system whose regulon includes three genes involved in LOS modification(12). PmrC and its orphan homologue, EptA, are transmembrane proteins able to add phosphoethanolamine to both the 1- and 4’ phosphate groups in lipid A (Fig. S2) (42). In addition, PmrAB positively regulates an operon including *naxD*, encoding a protein involved in the modification of the 1- phosphate group of lipid A via the addition of galactosamine (14).

To confirm that resistance in the *pmrB* mutants was due to modifications associated with upregulation of these genes, qRT-PCR analysis was performed. The transcript levels of *pmrC, eptA* and *naxD* were all increased in both *pmrB* mutants, with *pmrB*(T235I) resulting in higher upregulation than *pmrB*(A236E) relative to WT (Fig. 4B). When LOS preparations were analyzed by TLC, both mutants showed high levels of modified lipid A compared to WT, but the migration patterns of the modified forms were not identical in the two *pmrB* mutant strains (Fig. 4C). Serendipitously, the previously characterized colistin-resistant ATCC17978 R2 strain has a *pmrB*(T235I) mutation that results in lipid A modification as a consequence of both PmrC and NaxD activity(14, 42). The LAC-4 *pmrB*(T235I) mutant showed a similar lipid A profile to this strain, providing further evidence that colistin resistance in these mutants results from these two types of lipid A modification (Fig. 4C).

Mutations in *pmrB* in *A. baumannii* and other Gram-negative bacteria have been associated with colistin heteroresistance, which can be confirmed by performing population analysis profiling (PAP)(54). This assay was performed with LAC-4 WT and the *pmrB* mutants, which revealed that *pmrB*(A236E) is heteroresistant due to its ability to form colonies at low frequencies at colistin concentrations 4-8X higher than the resistance breakpoint, even though the MIC is considerably lower than the breakpoint(18, 54) (Fig. 4D). In contrast, the WT was unable to grow at 1μg/mL colistin, which was 4-fold below the clinical breakpoint. The *pmrB*(T235I) mutant was distinct from both these strains, as it had 100% colony-forming efficiency up to 64μg/mL colistin (Fig. 4D). PAP of the $LOS^{(-)}$ strains provided further evidence that the suppressor mutants have higher levels of colistin resistance compared to their $lpxA^{*}$ parent (Fig. 4D). Therefore, the *pmrB* mutant selected in the immune-depleted host (T235I) was colistin-resistant while the one selected in the immunocompetent host (A236E) was colistin

heteroresistant. Notably, in contrast to the high resistance strain, the heteroresistant mutant had a doubling time that was similar to WT during growth in broth culture (Fig. 2A).

Insertion sequences drive heteroresistance of the *pmrB*(A236E) strain.

Antibiotic heteroresistance is associated with strains that have subpopulations with higher levels of drug resistance relative to the parental strain(18). The high resistance exhibited in these subpopulations is often unstable and has been attributed to transient DNA amplification that allows hyperproduction of proteins that drive increased drug resistance(22). Consistent with this model, colistin heteroresistance in *Salmonella typhimurium* is driven by amplification of the *pmrD* gene, which encodes a positive regulator of *pmrAB*(24), and is consequently unstable via homologous recombination. *A. baumannii* does not encode *pmrD*, and little is known about what causes colistin heteroresistance in this organism other than it being linked to activating *pmrAB* mutations that drive upregulation of lipid A modifying enzymes(17). Therefore, starting with the low resistance *pmrB*(A236E) strain, we selected for increased resistance followed by continued growth in the absence of colistin selection to: 1) identify the genetic basis of variants that show high colistin-resistance in this strain; 2) test the stability of the resistant variants in the absence of colistin(18).

Three separate lines of the *pmrB*(A236E) strain were grown for 24 hours in LB broth supplemented with either 2μg/mL (Fig. 5A) or 4μg/mL (Fig. 5B) colistin, which were then passaged for 7 days in the absence of antibiotics. After drug exposure, colony forming efficiency (CFE) at 16μg/mL colistin increased to close to 100% frequency from the initial ~$5x10^{-4}$ CFE before drug exposure, demonstrating enrichment for the colistin-resistant subpopulation. Once colistin was removed, 5/6 tested lines retained their high CFE at 16μg/mL colistin after 7 days of passaging (Figs. 5A, B). These results demonstrate that colistin treatment selects for the resistant

subpopulation derived from the *pmrB*(A236E) strain that largely remains stable in the absence of antibiotic.

To detect genetic changes in the resistant *pmrB*(A236E) population, single colonies grown at 16μg/mL colistin were collected from all lines after 24 hours colistin treatment (day 0), and at 4 and 7 days after continuous passage in the absence of drug (Figs. 5A, B). E-test strips revealed that all 18 isolates had increased their colistin MIC compared to their *pmrB*(A236E) parent with 10/18 surpassing the breakpoint for clinical resistance (Table S1, COL MIC). Short-read whole genome sequencing was performed on a single colony from each timepoint, and confirmed they all retained the *pmrB*(A236E) mutation (Table S1; Materials and Methods). Surprisingly, only 5/18 isolates contained additional mutations detected through short-read sequencing and only 1/18 exhibited evidence of genome amplification, which was a 9 gene region not known to be associated with antibiotic resistance (Table S1 and Dataset S3).

Short-read sequencing analysis often fails to detect large insertions or other rearrangements in the genome(55). Long read sequencing and de-novo chromosomal assembly of the 18 isolates revealed that 17/18 isolates had acquired 1-4 insertion sequences (IS) at sites not found in the *pmrB*(A236E) parent (Table S1 and Dataset S3). Long-read sequencing also revealed that the high resistance *pmrB*(T235I) strain contained the additional insertion mutations (ABLAC_16720::IS*Aba25*, ABLAC_23900::IS*Aba1*, and ABLAC_35150::IS*Aba13*) absent in the WT ancestor (Dataset S3 and Fig. S3B).

The *A. baumannii* IS*Aba* insertion sequences are simple mobile genetic elements that can cause mutations by gene inactivation or altering expression patterns of transcripts downstream from transposition sites(56). The LAC-4 reference genome contains 6 different types of IS*Aba* inserted at 81 locations, comprising approximately 2.75% of the chromosome(36). IS*Aba*

insertions into the region upstream of *eptA* and gene-inactivating insertions in *hns* have been observed in colistin-resistant *A. baumannii* isolates, both resulting in increased *eptA* transcription(15, 16). Consistent with insertions in these regions causing increased resistance, 16/18 of the colistin-selected *pmrB*(A236E) isolates contained IS*Aba* insertions upstream of *eptA* or in the *hns* region (Figs. 5C, D; Figs. S4C, D; Table S1, and Dataset S3). qRT-PCR analysis of *eptA* expression in representative isolates confirmed that IS*Aba* transposition at either site increased *eptA* expression but not that of *pmrC* or *naxD* (Figs. 5E, F; Figs. S4C, D). Interestingly, several of the insertions upstream of *eptA* resulted in significantly lower expression of *naxD*, consistent with galactosamine modification of lipid A not being a critical determinant of increased colistin-resistance (Fig. S4C)(12). TLC profiling of selected colistin-resistant isolates showed similar lipid A profiles compared to the heteroresistant parental *pmrB*(A236E) mutant (Fig. S5). Thus, the stable colistin-resistant *pmrB*(A236E) subpopulation is predominantly created through IS*Aba* transposition events resulting in increased *eptA* expression.

Insertion mutations remain stable in the absence of colistin treatment.

The current models on heteroresistance postulate that the phenotypic stability of high drug resistance variants depends on the severity of the fitness cost of second-step mutations (18). The A-0-Hi isolate containing a single IS*Aba*25 insertion upstream of *hns* was chosen for further studies because it is the only second-step mutation identified in the *pmrB*(A236E) background that was associated with rapid loss of colistin resistance after subculture in the absence of drug (Fig. 5D; Fig. S6A and Dataset S3). qRT-PCR confirmed that the upstream insertion decreases *hns* gene expression in the A-0-Hi isolate compared to the *pmrB*(A236E) parent strain (Fig. S6 B). To test the stability of colistin resistance in this mutant, three separate lines of this A-0-Hi isolate were passaged for 14 days in the absence of antibiotic (Fig. 6A). Colony forming

efficiency at 16μg/mL colistin remained stable for 9 days (~120 generations), then decreased to *pmrB*(A236E) levels between days 10-14 (Fig. 6A). Therefore, we were unable to reproduce the instability seen in the *pmrB*(A236E) Col Hi, line A after passaging in antibiotic-free media (Fig. 5B). However, *pmrB*(A236E) A-0-Hi was a single high-frequency isolate collected from this line and may not accurately represent the potentially mixed population that lost resistance.

Isolates from all three lines were collected at day 14 from LB plates supplemented with 16 or 0 μg/mL colistin to identify the genetic changes that resulted in loss of resistance (Fig. 6A). Population analysis profiling confirmed that A-0-Hi colonies collected at day 14 from colistin-free plates, which we will refer to as pseudorevertants, had colistin sensitivity near WT levels and lower than their heteroresistant *pmrB*(A236E) ancestor (Fig. 6B). All A-0-Hi isolates collected at day 14 (either pseudorevertants or those remaining resistant) retained the IS*Aba25* insertion near *hns*, indicating that simple excision of the element was not the cause of the loss of drug resistance (Fig. S7). Rather, linear amplicon sequencing of the *pmrCAB* region revealed that all 18 colistin-sensitive pseudorevertants acquired new mutations disrupting either the *pmrA* or *pmrB* genes (Fig. 6C, Table S2).

To test whether reversion to sensitivity was due to the fitness cost incurred by high colistin resistance, growth rates in the absence of colistin were measured for the A-0-Hi strain and representative pseudorevertants (Fig. 6D, Fig. S8A). Only one pseudorevertant exhibited a significant decrease in doubling time compared to its A-0-Hi parent, with none reaching WT growth rates (Fig. 6D). During the continuous passaging experiment, cultures were grown for hours in post-exponential phase prior to subculturing (Fig. 6A), so we reasoned that the pseudorevertants may have a competitive advantage after exponential growth. Therefore, we performed 1:1 competition experiments with all seven pseudorevertants against their A-0-Hi

parent in LB broth and measured the competitive indices at 3 hours (mid-exponential) and 24 hours of culture (stationary). All pseudorevertants outcompeted their colistin-resistant parent at 24 hours, while none did so after 3 hours of culture (Figs. S8B, C). Thus, colistin resistance in the *pmrB*(A236E) A-0-Hi insertion mutant is stable, but continuous passaging in the absence of drug eventually selects for colistin-sensitive pseudorevertants, with loss-of-function mutations in *pmrAB* being a common source of the selective advantage (Fig. 6C).

Discussion:

In the murine pneumonia model, immune depletion results in a permissive environment for *A. baumannii* replication, facilitating the emergence and selection of tolerant and drug-resistant mutants that fail to reach high numbers in immunocompetent animals(33). We provide further evidence that immune depletion accelerates the emergence of antibiotic resistance, with mutants having altered colistin sensitivity arising more readily in the immune-depleted passages. Furthermore, we found that bacterial fitness was another important determinant of resistance evolution during infection, as highly colistin-resistant mutants lacking LOS(49) lost the ability to colonize both immunocompetent and immune-depleted mouse lungs even if they acquired secondary mutations that suppressed their growth defect in broth (Figs. 3C, E). The inability of $LOS^{(-)}$ mutants to colonize the host, even after they acquire suppressor mutations, is heartening because LPS/LOS-targeting antibiotics that select for loss of LPS are likely to prevent proliferation during disease(57). Altogether, these findings highlight the role of the host tissue environment and the innate immune response in restricting the selection pool of antibiotic-resistant variants(46).

Regardless of the host state, colistin treatment during pulmonary disease selected for mutations that increased the expression of enzymes modifying LOS, with *pmrB* transcription-activating mutants being enriched in our model, as previously observed in broth culture models and in clinical isolates(58) (Figs. 1C, D). The evolved *pmrB* mutants were outcompeted by their drug-sensitive parent during lung infections of immunocompetent mice but not in immune-depleted hosts (Figs. 2B, C). Unlike the LOS$^{(-)}$ mutants, both *pmrB* mutants retained the ability to grow in host tissues, allowing efficient competition with parental strains during colistin treatment (Figs. 2D, E). A previous study provided evidence that modified LOS from *A. baumannii pmrB* mutants induces higher TLR4 activation compared to unmodified LOS(59). This may be related to reports that some *pmrB* mutants have increased virulence, perhaps as a consequence of increased pattern recognition-driven inflammation(60, 61). Further work is needed to determine how LOS modifications caused by *pmrB* mutations impact the pathogenesis of *A. baumannii*.

We found that strains having mutations located one residue apart in the PmrB histidine kinase domain resulted in very different phenotypes (Fig. 4). Both mutants accumulated modified lipid A, with the doubly modified forms found at increased levels in the high resistance *pmrB(*T235I) strain compared to the heteroresistant *pmrB*(A236E) strain (Fig. 4C). This correlates well with the higher expression of *pmrC*, *eptA,* and *naxD* resulting from the *pmrB*(T235I) mutation (Fig. 4B). The high-resistance *pmrB*(T235I) mutant, however, was found to have three insertion element mutations that were absent both in the WT parent and the *pmrB*(A236E) strain (Dataset S3; COL17 vs. COL23), possibly explaining these resistance differences. When the *pmrB*(T235I) allele was backcrossed into WT LAC-4, the resulting strain had a colistin MIC (4μg/mL) that reached the clinical breakpoint for resistance, which is 8X

higher than that of both the backcrossed and evolved *pmrB*(A236E) mutant strains (Fig. S3A). Population analysis profiling showed that both the evolved and backcrossed *pmrB*(T235I) strains were able to form colonies all the way up to 64μg/mL colistin, with the evolved strain having a higher colony forming efficiency at this concentration as predicted by its higher E-test colistin MIC. In both backcrossed *pmrB* strains, an additional IS*Aba13* insertion was detected in identical locations and orientation 61bp upstream ABLAC_20540 (Dataset S3). Since this mutation does not confer resistance to the heteroresistant *pmrB*(A236E) backcrossed strain (Figure S3), we can reasonably conclude that the *pmrB*(T235I) allele is responsible and sufficient for conferring LAC-4 with colistin-resistance. Two additional IS*Aba* insertions mutations were detected in the backcrossed *pmrB*(A236E) strain; underscoring the remarkable plasticity of the LAC-4 genome. These results indicate that *pmrB* mutations located one residue apart can lead to either colistin resistance or heteroresistance.

Although the resistance level of the *pmrB*(T235I) backcrossed strain was above the clinically defined breakpoint, it is notable that mouse passaging selected for a strain with even higher levels of resistance, possibly due to the three additional IS insertions (Fig. S3A, COL17; MIC =16μg/mL). Evolved strains with the *pmrB*(T235I) mutation that harbored two of these insertion mutations (strains COL29-31) exhibited only a mildly increased MIC compared to the backcrossed mutant (Fig. S3A) and did not outcompete the population during mouse passage (Dataset S1; Figs. S1, S3). The third mutation, found only in the highest resistance isolate, was in ABLAC_23900, encoding a putative TetR family regulator (Fig. S3B). This triple insertion strain showed a 3X increase in *hns* expression compared to WT (Fig. S6C), which could be attributable to any of these insertions, including one located 513bp upstream of *hns* (ABLAC_35150::IS*Aba*13; Fig. S6A). Coupled with our data showing that increased *eptA*

expression is associated with insertions having decreased *hns* expression (Figs. 5E, S6B), it is possible that misregulation of *hns* in any direction could increase colistin resistance via *eptA* overexpression, which is clearly a key step in the progression to colistin resistance.

A confounding factor in the colistin resistance literature is that mutations in *pmrB* have been associated with colistin susceptibility, resistance and heteroresistance(54). Indeed, our heteroresistant *pmrB*(A236E) mutation has been previously associated with colistin resistance(43). Based on the IS*Aba* insertions that we identified, the possibility emerges that colistin-resistant *pmrB*(A236E) strains may have secondary mutations that activate *eptA* expression. This is because the accumulation of added IS*Aba* insertions in the genome can be easily missed, even when performing whole-genome sequencing(55). This raises the possibility that heteroresistance-conferring mutations like *pmrB*(A236E) present a double danger, because their "susceptible" classification results in improper antibiotic treatment that is both toxic for the patient and selects for higher resistance mutants. We do not believe that the selection of these second-step insertion mutations is a phenomenon of growth in culture, as we were able to identify similar insertion mutations in *pmrB*(A236E) isolates after continued passage in the colistin-treated murine pneumonia model (Figs. 2D, E; Fig. S9).

IS*Aba* transposition has been previously implicated in generating colistin-resistant isolates(19, 51, 59). It has been well-documented in several bacterial species that H-NS preferentially binds to chromosomal regions that are AT-rich relative to the rest of the genome(63). In *A. baumannii*, H-NS was shown to direct IS*Aba* transposition to these regions(62). Notably, the region upstream of *eptA* in LAC-4 is highly AT rich (79%) compared to the chromosome (61%), possibly explaining why 11/18 resistant isolates derived from *pmrB*(A236E) had IS*Aba* insertions in this region (Fig. 5C and Dataset S3) (16). In contrast, the

hns gene itself, where 4/18 *pmrB*(A236E) high resistance isolates had insertions, is only 64% TA, but the upstream intergenic region is 80.9% TA (Dataset S3).

Most of the isolates derived from the heteroresistant *pmrB*(A236E) strain had IS*Aba* insertions in additional sites in the chromosome with unknown contributions to resistance (Dataset S3). One hotspot was in an intergenic region (ABLAC_36890-ABLAC_36900) that contained IS*Aba25* insertions in 6/18 *pmrB*(A236E)-derived isolates (Fig. S10A). This region was also TA-rich (79%) and was flanked by genes involved in capsule synthesis (Dataset S3). Importantly, 5/6 of these isolates contained insertions in the vicinity of *eptA* and *hns* with the remaining isolate containing *eptA*(R127H) and *clpS*(Q90*) mutations that could contribute to colistin resistance (Figs. 5C, D; Dataset S3). The expression of the genes flanking these insertion mutations was tested via qPCR in two representative *pmrB*(A236E)-derived isolates, which contained either an *eptA*- or *hns*-disrupting insertion. In both isolates, the downstream gene ABLAC_36890 (annotated as *weeH*) had a significant (2X) reduction in expression while the upstream gene ABLAC_36900 only had increased expression when *hns* was disrupted (Figs. S10B, C). Mutations upstream of *weeH* are associated with changes in the colony morphology, capsule, biofilm and motility of the mutant(62). The high frequency of transposition events observed in this study highlights the potential role of insertion elements in the adaptability of *A. baumannii*.

After ~120 generations of growth in broth, the colistin-resistant *pmrB*(A236) A-0-Hi strain was outcompeted by colistin-sensitive pseudorevertants (Fig. 6A, B). The majority of these pseudorevertants acquired loss-of-function mutations in *pmrB*, mainly in the region encoding the histidine-kinase like ATPase domain (Fig. 6C, Table S2)(64). Other studies have observed colistin-resistant *A. baumannii* regain sensitivity after cessation of colistin therapy(11, 65).

Previously characterized colistin-sensitive pseudorevertants with mutations disrupting the *pmrCAB* operon included isolates that may have been evolutionary dead ends, because they produced colistin-resistant mutants at significantly lower frequencies than their WT ancestors (65). There are several physiological changes in these revertants that could affect both fitness in culture and colonization in the host. Deletion of *pmrA* and *pmrB* in *A. baumannii* reduces motility, the production of biofilm, and the generation of outer membrane vesicles(66). In mouse models, transposon insertion mutations in *pmrAB* are colonization-proficient, indicating that loss-of-function of the regulator is compatible with maintenance of virulence (67, 68). It is not clear, however, if PmrAB inactivation provides an advantage during disease only when such isolates compete against strains that constitutively activate the system.

In summary, we have presented evidence that growth of the heteroresistant *pmrB*(A236E) parent in colistin selects for insertion mutations that drive acquisition of resistance (Figs. 5C, D, Table S1, and Dataset S3). Similar insertion mutations can be selected after colistin treatment of lungs infected with the *pmrB*(A236E) strain (Figs. 2D, E; Fig. S9), or by simply incubating cultures of this heteroresistant mutant on agar plates supplemented with high colistin concentrations (Fig. S11). Based on the results presented in this study, we propose the following model. Strains having heteroresistance mutations, such as *pmrB*(A236E), create a heterogenous population with varying degrees of lipid A modifications (Fig. 7A). This enables a subpopulation to survive colistin challenge, potentially creating a stress condition that activates transposition and results in resistance through insertions in the *eptA* or *hns* regions (Fig. 7B). After cessation of antibiotic treatment, colistin-sensitive pseudorevertants can emerge that acquire mutations disrupting *pmrAB* (Fig. 7C). Although this model predicts that the *pmrB*(A236E) isolates with resistance-conferring secondary mutations should show an increase in LOS modification relative

to the *pmrB*(A236E) parent, this was not observed using the TLC strategy described here (Fig. S5). This technique does not quantify the relative abundance of each type of single/modified lipid A form, such as double-modified phosphoethanolamine versus singly modified galactosamine plus phosphoethanolamine, which we suspect may underly increased colistin resistance (Fig. 7B).

This work demonstrates that evolution of bacterial pathogens is a fine interplay between acquisition of antibiotic resistance and retention of fitness during growth and survival in tissues. As multidrug-resistant organisms continue to proliferate in healthcare and agricultural settings, accurately assessing the fitness costs of resistance mechanisms is crucial for identifying potential Achilles' heels for novel treatments. Our work and others point to phosphoethanolamine transferases (ex. PmrC/EptA), which can spread through horizontal gene transfer in *mcr* plasmids(69), as attractive drug targets due to their involvement in colistin resistance and heteroresistance(70). Furthermore, IS transposition should be considered when studying antibiotic heteroresistance mechanisms that cannot be explained by gene amplification(22). Lastly, our results support the model that *A. baumannii* LOS$^{(-)}$ mutants incur devastating fitness costs that prevent effective colonization during disease, highlighting the crucial role of this component in maintaining envelope integrity in Gram-negative bacteria(71).

Materials and Methods:

Bacterial strains. All strains of *Acinetobacter baumannii* (AB) are derivates of LAC-4 or ATCC17978UN(38, 72). Bacteria were grown in Lysogeny Broth (LB) or LB agar plates at 37°C. Broth cultures were grown in tubes and placed on a rotating roller drum set to 56rpm. Bacterial culture density was determined at 600nm (OD_{600}) using a cuvette and multiwell

spectrophotometer (Biotek Synergy) to monitor growth. Frozen stocks were prepared to a final glycerol concentration of 25% and stored at -80°C.

Molecular cloning and mutant construction. The *pmrB*(T235I) and *pmrB*(A236E) mutations were backcrossed from the COL17 and COL23 strains, respectively, into the parental LAC-4 WT background. This was accomplished by electroporation and plasmid integration followed by homologous recombination, as described previously(73). The mutant alleles were amplified from COL17 and COL23 to generate fragments of 2999 bp and cloned into pJB4648APRA, a suicide plasmid encoding apramycin resistance (Apra^{R}) derived from pSR47S(74). The plasmids harboring the mutant alleles were then integrated *via* homologous recombination into *A. baumannii* LAC-4, selecting Apra^{R} to generate heterozygotes. The resulting strains were then plated on LB+10% Sucrose at 30°C to select against the plasmid *sacB* allele, and screened for Apra^{S}. Recombinants that acquired the mutant *pmrB* allele were verified by sequencing amplified PCR products covering the *pmrB* region.

Measuring growth rate and competitive index in broth culture. Overnight cultures of denoted strains were diluted 1:1000 in fresh LB broth in tubes. Cultures were grown at 37°C in a rotating roller set to 56rpm. OD_{600} was measured at t=0, and at one hour time intervals through 6-8 hrs. 2-3 biological replicates (cultures derived from distinct colonies), each the average of 2 technical replicates (biological replicate diluted into separate cultures), were performed per strain. The averaged log_{10} values ± SEM over time were plotted. Doubling time of each biological replicate was calculated using a previously published script(https://github.com/huoww07/calulate_bacteria_doubling_time) (33). Mean doubling time and SEM of 2-3 biological replicates was calculated (Fig. 2A, 3C and 6D).

For competition experiments in broth, overnight cultures of denoted strains were adjusted to the same OD, mixed at an approximate 1:1 ratio and diluted into LB broth to a final OD of 0.002. Cultures were grown at 37°C in a rotating roller set to 56rpm. To calculate the ratio of the competing strains at denoted timepoints, aliquots of the cultures were 10X serially diluted and incubated on LB plates in presence or absence of colistin. The antibiotic concentration of the drug-supplemented plates was selected so that the colistin-resistant A-0-Hi strain, but not WT and the colistin sensitive pseudorevertants, were able to grow. 8μg/mL colistin was used for *pmrB*(A236E) A-0-Hi strains. Colistin resistance (ColR) strain CFU was determined by colonies on the antibiotic-containing plates, with Colistin sensitive (ColS) strain CFU = CFU on LB plate – CFU on antibiotic-containing plate. Competition Index (CI) = output(ColS/ColR) / input(ColS/ColR). Geometric Mean CI (each derived from individual cultures) and SD was plotted (Figs. S7A, B).

Selection of LOS deficient mutant and suppressors. Selection for a LOS deficient mutant was performed as described (32, 75). Overnight cultures of LAC-4 WT were diluted in LB and grown to mid-exponential phase. 10^9 CFU were then spread on 150mm LB plates that were supplemented with 10μg/mL colistin sulfate (Sigma: PHR1605). Slow-growing colonies that emerged at days 2 and 3 post-inoculation were picked and streaked on colistin-containing plates (10μg/mL) and grown overnight at 37°C. Only one of the picked colonies was able to grow at colistin 10μg/mL. This isolate and a LAC-4 WT control were then streaked on LB plates in presence or absence of 10μg/mL vancomycin (Sigma: SBR00001), and the colistin-resistant isolate was unable to grow in presence of vancomycin, as predicted for having a defect in LOS biosynthesis.

Mutants that improve fitness of the LOS deficient ($LOS^{(-)}$) strain were identified in the following fashion(27). The $LOS^{(-)}$ strain was grown to exponential phase, and 10^9 CFU was spread unto LB agar plates. These plates were incubated at 42°C for 3 days. At day 3, a lawn had formed, papillae were identified, streaked on LB plates and grown at 42°C overnight. The $LOS^{(-)}$ strain in the absence of temperature selection was streaked in parallel as a control. The following day, 18 of the purified papillae whose growth was visibly better than their $LOS^{(-)}$ parent were grown in LB and frozen at -80°C in 25% glycerol for downstream analysis.

Animal protocols. All animal procedures were approved by the Institutional Animal Care and Use Committee (IACUC) of Tufts University. All animals used in this study were 8-10 week-old female BALB/C mice obtained from Jackson Laboratories. All mice were housed in ventilated caging systems (10–15 air changes per hour) at temperatures of 68–79 °F (~20–26 °C) and 30–70% humidity, with 12 hr. light and dark cycle.

Bacterial passaging in pulmonary infection model. All passaging procedures were performed in identical manner in both the immunocompetent and immune-depleted mice, with inocula adjusted as described in Results(33). Immune depletion was induced by the intraperitoneal injection of 150mg/kg and 100mg/kg of cyclophosphamide monohydrate (Sigma: C7397) at days 4 and 1 prior to infection respectively(76). Lung infections were established by transiently anesthetizing mice through isoflurane inhalation followed by administering bacteria grown to mid-exponential phase (~$10^{\wedge 8}$ CFU for immunocompetent and ~$5x10^{\wedge 7}$-$5x10^{\wedge 6}$ CFU for immune-depleted mice) via oropharyngeal aspiration(33, 77). For the first passage, all three lines were derived from separate colonies and each line was maintained separately throughout the passaging. At 4hrs. post infection, mice were anesthetized with isoflurane and 8mg/kg colistin sulfate (Sigma: PHR1605) was directly administered into the trachea using a liquid PenWu

device (BioJane)(78). At 24-hours post infection, mice were sacrificed using CO_2, lungs were aseptically removed, then placed in ice-cold phosphate buffer saline (PBS) until they were processed with a tissue homogenizer (Omni). Lung bacterial burden (CFU/lung) was determined by performing 10-fold dilutions of lung homogenate on LB plates (Figs. 1B, C).

To outgrow LAC-4 (ciprofloxacin-resistant) and select against normal lung flora, the homogenate was plated on 150 mm LB agar plates containing 2μg/mL ciprofloxacin (Sigma: PHR1044) and incubated at 25°C overnight. The next day, the bacteria were scraped off the plates and resuspended in PBS to create 25% glycerol frozen stocks, or aliquoted into cryotubes stored at -80°C to be used for DNA purification.

For passage 2-16, the frozen bacteria from the previous passage were thawed, diluted in fresh LB, and grown to mid-exponential phase at 37°C. These cultures were then adjusted to the appropriate OD_{600} and used to create inocula containing the same approximate number of bacteria, differing by immune state as described above. The infection, drug administration, and bacterial harvest were performed in identical fashion at each passage (Fig. 1A).

The same protocol was used for competitions between purified LAC-4 mutants and WT in the presence of colistin treatment in either immunocompetent or immune-depleted mice (Figs. 2D, E). The mutants and WT were grown to mid-exponential phase, mixed at an approximate 5:95 ratio (mutant:WT), and inoculated into mice. Colistin treatment and lung processing was performed as described above. After overnight growth, the bacteria were collected and saved for the next round of infections. Mutant abundance versus WT (colony forming efficiency; CFE) was determined by plating frozen stocks in LB plates with or without colistin. The colistin concentrations (2μg/mL for *pmrB*(A236E) and 8μg/mL for *pmrB*(T235I) of the drug-supplemented LB plates ensured only the mutants and not WT could grow. Mutant abundance

was calculated by quantifying number of colonies growing in drug plate (selective for *pmrB* mutants) over number of colonies in no drug plate and then multiplied by 100. (Figs. 2D, E).

Mouse competition assays. Mouse competitions were performed as described(33). Immune depletion was induced with cyclophosphamide pre-treatment and infections were initiated via oropharyngeal aspiration (~$1X10^8$ CFU for immunocompetent group and ~$5x10^6$ CFU for immune-depleted group). At 24-hours post-infection, lungs were removed and homogenized aseptically in PBS. To calculate the ratio of the mutants to WT in both the inocula and the lung homogenates, the bacteria were 10X serially diluted and incubated on LB plates in presence or absence of colistin. The antibiotic concentration of the drug-supplemented plates was selected so that the mutants, but not the WT, were able to grow. 2μg/mL colistin was used for *pmrB*(A236E) and the LOS-deficient mutants, 8μg/mL was used for the *pmrB*(T235I) mutant, and 10ug/mL gentamycin was used to select against the gentamycin susceptible Δ*pABLAC2* mutant (Figs. 2B and 6E). Mutant CFU was determined by colonies on the antibiotic-containing plates, with WT CFU = CFU on LB plate – CFU on antibiotic-containing plate. Competition Index (CI) = output(Mutant/WT) / input(Mutant/WT). Geometric Mean CI (each derived from individual mouse infections) and SD was plotted (Figs. 2B, C; 3D, E).

Isolation and quantification of mutants with altered colistin susceptibility. Pools from each passage of the pulmonary infection model (Fig. 1B) were thawed and CFU were determined on LB plates in the absence of antibiotics and on graded concentrations of colistin (0.5μg/mL, 1μg/mL, 2μg/mL, 4μg/mL)(33). Colony forming efficiency (CFE) = number of colonies on colistin-containing plate/number of colonies in LB plate. For each colistin concentration tested, CFE was plotted as a function of passage number (Figs. 1C; S1).

Isolates, including the mutants characterized in this study, were purified and saved using the following protocol. Colonies from pools growing at a colistin concentration above that tolerated by WT were picked and re-streaked in LB colistin plates of the selected concentration. After overnight growth at 37°C, purified colonies were grown in LB broth and saved in 25% glycerol for downstream analysis. Only isolates able to grow and form isolated colonies at the selected colistin concentration were analyzed (Dataset S1, Table S1).

Population analysis profiling (PAP). Overnight cultures of LAC-4 WT and denoted mutants were diluted into fresh LB and grown to exponential phase. CFE were then determined on LB plates with increasing concentrations of colistin (0.5, 1, 2, 4, 8, 16, 32, 64 μg/mL)(54). CFE were plotted as a function of colistin concentration for each strain (Figs. 4C, 6B; Figs. S3C, S11B).

Antibiotic MIC determination. Polymyxin class antibiotics bind to the Costar plates(79), so colistin MIC determinations were performed using the E-test strip method(54). Overnight cultures of WT and mutants were diluted into fresh LB broth, grown to exponential phase, and adjusted to an OD_{600} = 0.1 in PBS (approximating 0.5X MacFarland standard). A sterile swab was used to apply the bacteria to LB plates and colistin E-strips (Biomerieux) were placed on top. Plates were incubated overnight at 37°C and MIC was determined by identifying the site where the zone of inhibition meets the strip (Figs. 3A, S3A, Table S1, Dataset S1).

Resistance stability assay. The resistance stability assay was performed as described(80). Three separate colonies of the *pmrB*(A236E) mutant were used to establish three lines. Overnight cultures for each line were grown in LB at 37°C. These cultures (input) were then diluted 1:100 in LB supplemented with either 2μg/mL or 4μg/mL colistin and grown for 24 hours at 37°C. After 24 hrs. drug exposure (Day 0), each culture was diluted 1:100 (Fig. 5A, B)

or 1:10,000 (Fig. 6A) into fresh LB broth without antibiotic and was grown for 24 hours. Cultures were identically passaged in the absence of antibiotic for 7 days (Figs. 5A, B) or 14 days (Fig. 6A). At each day (input, day 0-7), colony forming efficiency at 16μg/mL colistin relative absence of drug was determined (Figs. 5A, B; Fig. 6A). For the *pmrB*(A236E) passaging, isolates able to grow at 16μg/mL colistin were collected from day 0, 4, and 7 for further genome sequencing (Table 1). For the A-0-Hi passaging, isolates from day 14 growing at 0 and 16μg/mL colistin plates were saved (Fig. 6A).

Quantification of transcription by qPCR. Overnight cultures of denoted strains were diluted into fresh LB and grown at 37°C until mid-exponential phase. RNA was extracted following manufacturer's instructions (Qiagen RNAeasy: 74106) and subjected to cDNA synthesis using the SuperScript IV VILO kit (Invitrogen: 11756050). The qPCR reactions were performed using the PowerUp SYBR Green Master Mix (Applied Biosystems: A25742) and were run on a StepOnePlus Real-Time PCR system (Applied Biosystems) following manufacturer's instructions. Transcript level of target genes were normalized to 16S ribosomal RNA and fold change compared to WT was calculated using the ΔΔCt method. Three biological replicates, with 2 technical replicates each, were performed per strain. The values were plotted as mean ± SEM (Figs. 3C; 4E, F; S4C, D; S6B, C; S10B, C).

Endpoint PCR. Colonies from denoted strains were resuspended in ultra-pure water and lysed by a 5-minute incubation at 95°C. Colony PCR was performed using the OneTaq 2X master mix reagents (NEB: M0482S) on a Biorad T100 thermal cycler following manufacturer's instructions. Primers used are listed in Table S4. PCR products were visualized on a Biorad Gel Dock Go imaging system after running on a 1% agarose TAE gel (Figs. S3B, S7, S9; Figs. S11A, C). The DNA 1kb Plus Ladder (Invitrogen: 10787018) was used as a reference. PCR

products were purified using the Qiaquick PCR purification kit (Qiagen: 28104). Denoted samples were sent to Plasmidsaurus for linear amplicon sequencing and mutations were detected by aligning sequences to the reference genome on Geneious Prime (Fig. 6C, Table S2).

Whole genome sequencing. Genomic DNA (gDNA) was purified from denoted isolates using the DNeasy blood and tissue kit (Qiagen: 69506). Illumina Nextera reagents were used to prepare the libraries for short-read sequencing as described(33). 100bp single-end reads were obtained from pooled libraries using either a HiSeq2500 or a NovaSeq X Plus at the Tufts University Core Facility (http://tucf-genomics.tufts.edu/). Mutations present above a 5% cutoff were identified by applying the BRESEQ 0.38.8 pipeline to align the reads to the LAC-4 reference genome, including chromosome and two plasmids(81). (GenBank Accession: chromosome CP007712, pABLAC1 CP007713 and pABLAC2 CP007714)(36). Mutations described in selected passaged strains are those not present in the ancestral LAC-4 WT strain. (Dataset S1, S2, S3). See Dataset S4 for a comprehensive list of mutations detected in the evolved isolates.

For long-read sequencing, library preparation and sequencing was performed by the Hartwell Center for Biotechnology at St. Jude Children's Hospital. gDNA samples were quantified using the Quant-It Pico Green dsDNA assay (Invitrogen) and quality was assessed by fragment size analysis using the Femto Pulse system with the Genomic DNA 165 kb kit (Agilent). Samples with a median size greater than 10 kb were sheared to 10 kb using Covaris g-Tubes in a volume of 150µl buffer (10 mM Tris pH 8.0, 0.1 mM EDTA). Four column passes at 6,000 rpm were performed (Eppendorf: 5424). Sheared DNA was concentrated by performing a 1:1 clean-up using SMRT beads (PacBio) and eluted in 46 µl of low EDTA TE. Samples with a median size of less than 10 kb were not sheared, and then brought up to 46 µl using the same

buffer. Libraries were individually constructed from 0.3 - 1 ug of genomic DNA using the TPK 3.0 library preparation kit (PacBio), including the addition of barcoded PacBio SMRTbell adapters to allow for multiplexing.

Up to 96 libraries were pooled in equimolar amounts and loaded onto a single Revio SMRT cell at a concentration of 250 pM. Sequencing run conditions were performed as follows: 1) adaptive loading turned on (target of 0.85); 2) base kinetics turned on; 3) two hr. pre-extension time; 4) 30 hr. movie time. Alternatively, gDNA was sent to Plasmidsaurus for Nanopore long-read sequencing. Sequencing reads were de-novo assembled into genomes/contigs using the CANU pipeline(82). Mauve whole genome alignments on Geneious Prime were performed to compare the chromosomes of the mutants versus their parent. Insertions and deletions present in the mutants but not the parent were then identified (Dataset S3). All sequencing information provided in this text has been deposited in Genbank under the accession number PRJNA1273616.

LOS and lipid A visualization. For fractionation and staining of whole cell LOS, 10^9 CFUs of denoted strains were collected, washed and resuspended in 1X LDS sample buffer + 5% β-mercaptoethanol, and boiled for 10 minutes. Samples were then treated with proteinase K and run on a 4-12% Bis-Tris SDS-PAGE gel. Staining of LOS was performed using the ProQ Emerald 300 (Thermo Fisher) kit, following manufacturer instructions (Fig. 3A) (83).

Lipid A isolation for TLC analysis from denoted AB strain was performed as described(83). Overnight cultures of denoted strains were diluted into fresh LB with 5 µCi/mL ^{32}P ortho-phosphoric acid (Perkin-Elmer) and grown to an OD_{600} = 1. Lipid A was extracted using mild-acid hydrolysis followed by a Blight-Dryer extraction. Lipid A species were separated by thin layer chromatography (TLC) in a chloroform/pyridine/88% formic acid/water

(50:50:16:5, vol/vol) solvent system. An Amersham Typhoon laser scanner with a phosphorimaging screen was used to image the dry plates (Figs. 3A, S5).

Statistical Analysis. GraphPad Prism was used for statistical analysis. For all statistical analysis, One Way ANOVA followed by Dunnet's multiple comparison or unpaired two-tailed t-tests were employed. *$P < 0.05$, **$P < 0.01$, ***$P < 0.001$, ****$P < 0.0001$; ns, not significant.

Figure Design. Illustrations in Figures 1A, 3B and 7 were created in BioRender.com.

Acknowledgements:

This work is supported by NIAID U01AI124302, U19AI158076, U19AI142780 and R21AI128328. We would like to thank Albert Tai and Irina V. Grinvald for help with library preparations and the next-generation sequencing support provided by S10OD032203 via Tufts University Core Facility Genomics Core. We would like to thank the St. Jude Children's Hospital Hartwell Center for Biotechnology for help with sequencing library preparation and Pacbio sequencing. We would like to thank Eddie Geisinger, Tim Van Opijnen and all the members of the Isberg lab for their feedback on the study.

Author Contributions:

J.H-B. and R.R.I devised the study. J.H-B., B.H., L.M.V., E.B.B. and G. I. C. T. performed the wet lab experiments. H.E. and J.M.R. performed long-red sequencing and provided consultation on library preparations. J.H-B and W.H. performed the sequencing analysis. L.M.V and M.S.T. performed the LOS analysis and provided analysis of results.

Figure Legends:

Figure 1: Colistin treatment selects for *pmrB* mutations in *A. baumannii* during serial oropharyngeal inoculations.

A. Passaging strategy. Immune depletion was induced by intraperitoneal (IP) cyclophosphamide injections at 72- and 24- hours before infection. Three separate, co-housed lines derived from different LAC-4 colonies were passaged per condition. *A. baumannii* LAC-4 was oropharyngeally (OP) inoculated into mice and 4 hours post-infection (hpi), 8mg/kg aerosolized colistin was administered via OP inhalation. At 24 hpi, the mice were euthanized, lungs were removed, homogenized, and plated on LB agar plates. After overnight growth, the bacteria were collected and saved for the next round of infections. **B-C.** Lung CFU after each passage in colistin-treated mice. Dotted line: expected bacterial burden in the absence of colistin treatment (Materials and Methods). At passage 2 in immune-depleted host, the inoculum size of $5X10^7$ CFU was reduced to $1X10^7$ CFU, followed by a reduction to $5X10^6$ CFU at passage 5 (arrows). Inoculum size in immunocompetent host: $1X10^8$ CFU. **D-E.** Identification of colistin-resistant mutants. Pools were serially diluted and plated on LB plates supplemented with 0 or 4 μg/mL colistin. Colony forming efficiency (CFE) was calculated by the ratio of colonies growing in the presence or absence of drug. Dotted line: limit of detection. Isolates that grew in colistin plates were whole-genome sequenced to reveal the presence of the noted *pmrB* mutations.

Figure 2: Mutations in *pmrB* selected during pulmonary infection incur a fitness cost in the absence of colistin.

A. Kinetics of *pmrB* mutant growth in broth. Denoted LAC-4 strains were incubated in LB broth, and mass increase was measured at one-hour intervals. Mean doubling time $\pm$ SEM of three biological replicates shown. **B-C.** Competition of *pmrB* mutants vs. WT during pulmonary infections. Denoted strains were mixed at approximately 1:1 and inoculated via oropharyngeal

aspiration into animals treated under noted conditions. 24hpi, mice were euthanized, and lungs were removed, homogenized in cold PBS, and plated on LB plates with or without colistin. Competition Index (CI) determined as described (Materials and Methods). Geometric Mean CI ± SD of 9-16 biological replicates was determined. **D-E.** The *pmrB*(T235I) strain efficiently competes with LAC-4 WT during pulmonary infections in the presence of colistin. LAC-4 WT and noted mutants were mixed at approximately 95:5 ratio followed by oropharyngeal inoculation into mice. 8mg/kg of colistin was administered 4hpi. At 24 hpi, the mice were euthanized, lungs were removed, homogenized, and plated on LB agar plates (Materials and Methods). Frozen pools from each passage were serially diluted and spot plated in LB plates supplemented with 0, 2 or 8μg/mL colistin. Mutant abundance was calculated as described (Materials and Methods). **A-C.** Statistical analysis of doubling time and CIs was performed using One-way ANOVA, followed by Dunnett's multiple comparisons (Materials and Methods). $*P < 0.05$, $****P < 0.0001$; ns, not significant.

Figure 3: LOS-deficient *A. baumannii* isolates are defective for lung colonization.

A. LOS$^{(-)}$ strains lack carbohydrate sidechain. LOS isolated from denoted strains was fractionated on SDS-PAGE and carbohydrate was stained with ProQ Emerald 300. The denoted *E. coli* strain does not produce O-antigen and should migrate closely to *A. baumannii* LOS. The bottom band present in all samples is an unknown glycolipid or intermediate species. **B.** Protocol for selection of LOS-deficient LAC-4 and high fitness variants. WT LAC-4 was plated on LB plates supplemented with 10μg/mL colistin and colonies were restreaked onto identical medium. An isolate (*lpxA**) that grew at 10μg/mL colistin but not 10μg/mL vancomycin was saved and sequenced. 10^9 CFU of the isolate were plated on LB at 42°C and papillae growing above the lawn after 72 hrs. were streaked onto LB. Candidates showing improved growth at 42°C relative

to parental LOS$^{(-)}$ strain were saved and sequenced (Dataset S2). Three non-identical isolates (*lpxA** *pldA**, *lpxA** *pldA** *pbp1A*^{ins}, and *lpxA** *pldA** *pbp1A**) were selected for further study. **C.** Kinetics of LOS$^{(-)}$ mutant growth in broth. Denoted LAC-4 strains were incubated in LB broth, and mass increase was measured at one-hour intervals. Mean doubling time ± SEM of replicates shown. **D-E.** Competition of LOS$^{(-)}$ mutants vs. WT during pulmonary infection. Denoted strains were mixed approximately 1:1 and inoculated via oropharyngeal aspiration into mice. 24hpi, mice were euthanized, lungs were removed, homogenized in cold PBS, and incubated on LB solid medium in presence or absence of colistin. Geometric Mean CI ± SD of 8-9 replicates determined as described (Materials and Methods). **C-E.** Statistical analysis of doubling time and CI's were performed using one-way Anova followed by Dunnett's multiple comparison. $^{**}P < 0.01$, $^{***}P < 0.001$; ns, not significant.

Figure 4: Overexpression of *pmrB*-regulated genes leads to colistin resistance and heteroresistance.

A. Susceptibility of *pmrB* and LOS^{-} mutants to colistin. Colistin MIC determination via E-test strip. MIC determined as described (Materials and Methods). **B.** Expression of *pmrAB*-regulated genes in colistin-selected *pmrB* mutants. Transcript levels of *pmrC, eptA and naxD* was quantified via RT-qPCR and displayed as expression relative to WT. Mean ± SEM from three biological replicates shown. **C.** Lipid A from denoted strains was isolated, radiolabeled with ^{32}P and separated by thin layer chromatography (TLC). Double modified form refers to the addition of phosphoethanolamine and/or galactosamine. **D.** Population analysis profiling of *pmrB* and LOS^{-} mutants**.** Cultures of denoted strains were serially diluted and plated in LB supplemented with noted concentrations of colistin. Mean colony forming efficiency (CFE) was calculated as described (Materials and Methods). Grey vertical line: clinical breakpoint for resistance

(≥4μg/mL). **B.** Statistical analysis of gene expression changes were performed using unpaired, two-tailed t-tests. ***$P < 0.001$.

Figure 5: Dynamics of high-resistance isolates having the *pmrB*(A236E) mutation during passage in the absence of antibiotic.

A-B. Enrichment and stability of high colistin resistance strains derived from the *pmrB*(A236E) background. Three lines (A, B, C) of the *pmrB*(A236E) mutant were selected for high resistance by 24 hr. growth in either 2μg/mL (Lo) or 4μg/mL (Hi) colistin (Day 0/+COL). Each line was subsequently passaged daily in antibiotic-free media for 7 days. Every 24 hrs., CFU were quantified and colony forming efficiency (CFE) on LB containing 16μg/mL colistin plates was determined, as described (Materials and Methods). Colonies growing at 16μg/mL colistin were isolated at day 0, 7, 14 for further analysis. **C-D.** Location and orientation of IS*Aba* insertions in colistin-enriched *pmrB*(A236E) isolates. Figures not drawn to scale. **E-F.** Expression of *eptA* in the colistin-enriched *pmrB*(A236E) isolates. Representative isolates (in bold) were selected for further analysis. Transcript levels of *eptA* in mutants relative to WT was quantified via RT-qPCR. Mean ± SEM from three biological replicates shown. **C-F.** Isolate nomenclature refers to "Line – Day collected – Level of colistin exposure at day 0". **E-F.** Statistical analysis of gene expression changes were performed using one-way Anova followed by Dunnett's multiple comparison. *$P < 0.05$, **$P < 0.01$, ****$P < 0.0001$.

Figure 6: Colistin-susceptible *pmrB*(A236E) A-0-Hi pseudorevertants emerge after continued passaging in the absence of drug.

A. Stability of colistin resistance in the absence of antibiotic selection. Three lines of the colistin-resistant *pmrB*(A236E) A-0-Hi isolate were passaged in antibiotic-free media for 14 days. Every 24 hrs, colony forming units on LB containing 16μg/mL colistin plates was measured. CFE was calculated as described (Materials and Methods). **B-D.** 18 *pmrB*(A236E) A-0-Hi pseudorevertants (PR) were collected for further analysis by picking colonies growing on LB plates after 14 days of antibiotic-free passaging. **B.** Population analysis profiling of *pmrB*(A236E) A-0-Hi pseudorevertants. Cultures of denoted strains were serially diluted and plated on LB agar supplemented with noted concentrations of colistin. CFE was calculated as described (Materials and Methods). **C.** Schematic indicating identity and location of mutations in representative *pmrB*(A236E) A-0-Hi pseudorevertants detected by linear amplicon sequencing of *pmrCAB* region. **D.** Growth rates of *pmrB*(A236E) A-0-Hi pseudorevertants in broth. Mean doubling time + SEM of three biological replicates shown. Statistical analysis of doubling time was performed using One-way Anova followed by Dunnett's multiple comparison. $*P < 0.05$, $****P < 0.0001$; ns, not significant. Kinetics shown in Figure S8A.

Figure 7. Model for the two-step acquisition of colistin resistance.

A. Activation of PmrB histidine kinase (via signal or mutation) leads to phosphorylation of PmrA. PmrA transcription factor binds to PmrA binding site in the *pmrCAB*, *eptA* and *naxD* promoter regions. PmrC and EptA add phosphoethanolamine (PEtN) to the 1 and 4’ phosphate groups on lipid A. NaxD deacetylates *N*-acetylgalactosamine (GalNAc) to galactosamine (GalN), which is then added to the 1- phosphate on lipid A by an unknown enzyme. These modifications reduce the negative charge of the lipid A portion of lipooligosaccharide which reduce its affinity to colistin. Mutations that strongly activate this system [ex. *pmrB*(T235I)] lead to resistance while mutations that weakly activate this system [ex. *pmrB*(A236E)] lead to heteroresistance. **B.**

Heteroresistant *pmrB* mutant becomes fully colistin-resistant through insertion sequence transposition. The *eptA* gene is poorly activated by the *pmrB*(A236E) mutation, as the upstream region is TA rich and is silenced by H-NS (Sensitive). IS*Aba* transposition to region upstream of *eptA* increases the expression of this gene leading to resistance (Path 1). IS*Aba* transposition into *hns* derepresses TA rich regions of the genome, including *eptA*, and leads to resistance (Path 2). **C.** Continued passaging in the absence of drug selects for colistin sensitive pseudorevertants that acquire loss of function mutations in *pmrAB*.

References:

1. Centers for Disease Control and Prevention (U.S.), "Antibiotic resistance threats in the United States, 2019" (Centers for Disease Control and Prevention (U.S.), 2019).

2. A. K. Cain, M. Hamidian, Portrait of a killer: Uncovering resistance mechanisms and global spread of Acinetobacter baumannii. *PLOS Pathogens* **19**, e1011520 (2023).

3. D. Wong, *et al.*, Clinical and Pathophysiological Overview of Acinetobacter Infections: a Century of Challenges. *Clinical microbiology reviews* **30**, 409–447 (2017).

4. C. Ayoub Moubareck, D. Hammoudi Halat, Insights into Acinetobacter baumannii: A Review of Microbiological, Virulence, and Resistance Traits in a Threatening Nosocomial Pathogen. *Antibiotics* **9**, 119 (2020).

5. WHO bacterial priority pathogens list, 2024: Bacterial pathogens of public health importance to guide research, development and strategies to prevent and control antimicrobial resistance. Available at: https://www.who.int/publications/i/item/9789240093461.

6. B. Isler, Y. Doi, R. A. Bonomo, D. L. Paterson, New Treatment Options against Carbapenem-Resistant Acinetobacter baumannii Infections. *Antimicrobial Agents and Chemotherapy* **63**, 10.1128/aac.01110-18 (2018).

7. D. Landman, C. Georgescu, D. A. Martin, J. Quale, Polymyxins Revisited. *Clinical Microbiology Reviews* **21**, 449–465 (2008).

8. A. L. H. Kwa, C. Loh, J. G. H. Low, A. Kurup, V. H. Tam, Nebulized Colistin in the Treatment of Pneumonia Due to Multidrug-Resistant Acinetobacter baumannii and Pseudomonas aeruginosa. *Clinical Infectious Diseases* **41**, 754–757 (2005).

9. Z. Zhang, *et al.*, The efficacy and safety of inhaled antibiotics for pneumonia: A systematic review and meta-analysis. *Pulmonary Pharmacology & Therapeutics* **86**, 102315 (2024).

10. J. H. Moffatt, M. Harper, J. D. Boyce, "Mechanisms of Polymyxin Resistance" in *Polymyxin Antibiotics: From Laboratory Bench to Bedside*, J. Li, R. L. Nation, K. S. Kaye, Eds. (Springer International Publishing, 2019), pp. 55–71.

11. M. D. Adams, *et al.*, Resistance to Colistin in Acinetobacter baumannii Associated with Mutations in the PmrAB Two-Component System. *Antimicrobial Agents and Chemotherapy* **53**, 3628–3634 (2009).

12. N. Yamada, *et al.*, PmrAB, the two-component system of Acinetobacter baumannii, controls the phosphoethanolamine modification of lipooligosaccharide in response to metal ions. *Journal of Bacteriology* **206**, e00435-23 (2024).

13. L. A. Arroyo, *et al.*, The pmrCAB operon mediates polymyxin resistance in Acinetobacter baumannii ATCC 17978 and clinical isolates through phosphoethanolamine modification of lipid A. *Antimicrobial agents and chemotherapy* **55**, 3743–51 (2011).

14. C.-Y. Chin, K. A. Gregg, B. A. Napier, R. K. Ernst, D. S. Weiss, A PmrB-Regulated Deacetylase Required for Lipid A Modification and Polymyxin Resistance in Acinetobacter baumannii. *Antimicrobial agents and chemotherapy* **59**, 7911–4 (2015).

15. E. J. Yoon, *et al.*, Trajectory of genetic alterations associated with colistin resistance in Acinetobacter baumannii during an in-hospital outbreak of infection. *Journal of Antimicrobial Chemotherapy* **77**, 69–73 (2021).

16. D. D. Lucas, *et al.*, Emergence of High-Level Colistin Resistance in an Acinetobacter baumannii Clinical Isolate Mediated by Inactivation of the Global Regulator H-NS. (2018). https://doi.org/10.1128/AAC.02442-17.

17. Y. Charretier, *et al.*, Colistin Heteroresistance and Involvement of the PmrAB Regulatory System in Acinetobacter baumannii. *Antimicrobial Agents and Chemotherapy* **62**, 10.1128/aac.00788-18 (2018).

18. D. I. Andersson, H. Nicoloff, K. Hjort, Mechanisms and clinical relevance of bacterial heteroresistance. *Nature Reviews Microbiology 2019 17:8* **17**, 479–496 (2019).

19. V. I. Band, D. S. Weiss, Heteroresistance: A cause of unexplained antibiotic treatment failure? *PLOS Pathogens* **15**, e1007726 (2019).

20. V. I. Band, D. S. Weiss, Heteroresistance to beta-lactam antibiotics may often be a stage in the progression to antibiotic resistance. *PLoS Biol* **19**, e3001346 (2021).

21. A. Pal, D. I. Andersson, Bacteria can compensate the fitness costs of amplified resistance genes via a bypass mechanism. *Nat Commun* **15**, 2333 (2024).

22. H. Nicoloff, K. Hjort, B. R. Levin, D. I. Andersson, The high prevalence of antibiotic heteroresistance in pathogenic bacteria is mainly caused by gene amplification. *Nature Microbiology 2019 4:3* **4**, 504–514 (2019).

23. K. N. Kang, *et al.*, Colistin heteroresistance in Enterobacter cloacae is regulated by PhoPQ-dependent 4-amino-4-deoxy-l-arabinose addition to lipid A. *Molecular microbiology* **111**, 1604 (2019).

24. K. Hjort, H. Nicoloff, D. I. Andersson, Unstable tandem gene amplification generates heteroresistance (variation in resistance within a population) to colistin in Salmonella enterica. *Molecular Microbiology* **102**, 274–289 (2016).

25. L. Bardet, *et al.*, Deciphering Heteroresistance to Colistin in a Klebsiella pneumoniae Isolate from Marseille, France. *Antimicrobial Agents and Chemotherapy* **61**, 10.1128/aac.00356-17 (2017).

26. S. P. Doijad, *et al.*, Resolving colistin resistance and heteroresistance in Enterobacter species. *Nat Commun* **14**, 140 (2023).

27. M. J. Powers, M. S. Trent, Phospholipid retention in the absence of asymmetry strengthens the outer membrane permeability barrier to last-resort antibiotics. *Proceedings of the National Academy of Sciences of the United States of America* **115**, E8518–E8527 (2018).

28. M. J. Powers, M. S. Trent, Expanding the paradigm for the outer membrane: Acinetobacter baumannii in the absence of endotoxin. *Molecular Microbiology* **107**, 47–56 (2018).

29. G. J. D. Silva, S. Domingues, Interplay between Colistin Resistance, Virulence and Fitness in Acinetobacter baumannii. *Antibiotics* **6** (2017).

30. J. Y. Lee, E. S. Chung, K. S. Ko, Transition of colistin dependence into colistin resistance in Acinetobacter baumannii. *Scientific Reports 2017 7:1* **7**, 1–11 (2017).

31. J. S. Hawley, C. K. Murray, J. H. Jorgensen, Development of colistin-dependent Acinetobacter baumannii-Acinetobacter calcoaceticus complex [1]. *Antimicrobial Agents and Chemotherapy* **51**, 4529–4530 (2007).

32. J. M. Boll, *et al.*, A penicillin-binding protein inhibits selection of colistin-resistant, lipooligosaccharide-deficient Acinetobacter baumannii. *Proceedings of the National Academy of Sciences of the United States of America* **113**, E6228–E6237 (2016).

33. W. Huo, *et al.*, Immunosuppression broadens evolutionary pathways to drug resistance and treatment failure during Acinetobacter baumannii pneumonia in mice. *Nat Microbiol* **7**, 796–809 (2022).

34. K. W. Bruhn, *et al.*, Host fate is rapidly determined by innate effector-microbial interactions during Acinetobacter baumannii bacteremia. *The Journal of infectious diseases* **211**, 1296–305 (2015).

35. A. Maure, E. Robino, C. Van der Henst, The intracellular life of *Acinetobacter baumannii*. *Trends in Microbiology* **31**, 1238–1250 (2023).

36. H.-Y. Ou, *et al.*, Complete genome sequence of hypervirulent and outbreak-associated Acinetobacter baumannii strain LAC-4: epidemiology, resistance genetic determinants and potential virulence factors. *Scientific Reports* **5** (2015).

37. S. C. Valentine, *et al.*, Phenotypic and Molecular Characterization of Acinetobacter baumannii Clinical Isolates from Nosocomial Outbreaks in Los Angeles County, California. *J Clin Microbiol* **46**, 2499–2507 (2008).

38. G. Harris, *et al.*, A Mouse model of acinetobacter baumannii-associated pneumonia using a clinically isolated hypervirulent strain. *Antimicrobial Agents and Chemotherapy* **57**, 3601–3613 (2013).

39. R. J. North, Cyclophosphamide-facilitated adoptive immunotherapy of an established tumor depends on elimination of tumor-induced suppressor T cells. *Journal of Experimental Medicine* **155**, 1063–1074 (1982).

40. A. F. Zuluaga, *et al.*, Neutropenia induced in outbred mice by a simplified low-dose cyclophosphamide regimen: characterization and applicability to diverse experimental models of infectious diseases. *BMC Infect Dis* **6**, 55 (2006).

41. MR01Ed2E | Polymyxin Breakpoints for Enterobacterales, Pseudomonas aeruginosa, and Acinetobacter spp., 2nd Edition. *Clinical & Laboratory Standards Institute*. Available at: https://clsi.org/standards/products/microbiology/companion/mr01/.

42. L. A. Arroyo, *et al.*, The pmrCAB operon mediates polymyxin resistance in Acinetobacter baumannii ATCC 17978 and clinical isolates through phosphoethanolamine modification of lipid A. *Antimicrobial Agents and Chemotherapy* **55**, 3743–3751 (2011).

43. R. López-Rojas, M. García-Quintanilla, G. Labrador-Herrera, J. Pachón, M. J. McConnell, Impaired growth under iron-limiting conditions associated with the acquisition of colistin resistance in *Acinetobacter baumannii*. *International Journal of Antimicrobial Agents* **47**, 473–477 (2016).

44. T. Vogwill, R. C. MacLean, The genetic basis of the fitness costs of antimicrobial resistance: a meta-analysis approach. *Evolutionary applications* **8**, 284–95 (2015).

45. A. H. Melnyk, A. Wong, R. Kassen, The fitness costs of antibiotic resistance mutations. *Evolutionary Applications* **8**, 273 (2015).

46. M. J. Culyba, D. V. Tyne, Bacterial evolution during human infection: Adapt and live or adapt and die. *PLOS Pathogens* **17**, e1009872 (2021).

47. B. W. Simpson, *et al.*, Acinetobacter baumannii Can Survive with an Outer Membrane Lacking Lipooligosaccharide Due to Structural Support from Elongasome Peptidoglycan Synthesis. *mBio* (2021). https://doi.org/10.1128/MBIO.03099-21.

48. J. W. Skudlarek, *et al.*, Cerastecin Inhibition of the Lipooligosaccharide Transporter MsbA to Combat Acinetobacter baumannii: From Screening Impurity to In Vivo Efficacy. *J. Med. Chem.* **67**, 15620–15675 (2024).

49. K. Novović, B. Jovčić, Colistin Resistance in Acinetobacter baumannii: Molecular Mechanisms and Epidemiology. *Antibiotics* **12**, 516 (2023).

50. R. López-Rojas, *et al.*, Impaired virulence and in vivo fitness of colistin-resistant Acinetobacter baumannii. *The Journal of infectious diseases* **203**, 545–8 (2011).

51. M. E. Wand, L. J. Bock, L. C. Bonney, J. M. Sutton, Retention of virulence following adaptation to colistin in Acinetobacter baumannii reflects the mechanism of resistance. *Journal of Antimicrobial Chemotherapy* **70**, 2209–2216 (2015).

52. A. Beceiro, *et al.*, Biological cost of different mechanisms of colistin resistance and their impact on virulence in Acinetobacter baumannii. *Antimicrobial agents and chemotherapy* **58**, 518–26 (2014).

53. S. Gerson, *et al.*, Diversity of amino acid substitutions in PmrCAB associated with colistin resistance in clinical isolates of *Acinetobacter baumannii*. *International Journal of Antimicrobial Agents* **55**, 105862 (2020).

54. E. X. Sherman, J. E. Wozniak, D. S. Weiss, Methods to Evaluate Colistin Heteroresistance in Acinetobacter baumannii. *Methods in molecular biology (Clifton, N.J.)* **1946**, 39 (2019).

55. N. D. Maio, *et al.*, Comparison of long-read sequencing technologies in the hybrid assembly of complex bacterial genomes. *Microbial Genomics* **5**, e000294 (2019).

56. H. R. Noel, J. R. Petrey, L. D. Palmer, Mobile genetic elements in Acinetobacter antibiotic-resistance acquisition and dissemination. *Annals of the New York Academy of Sciences* **1518**, 166–182 (2022).

57. C. Zampaloni, *et al.*, A novel antibiotic class targeting the lipopolysaccharide transporter. *Nature* **625**, 566–571 (2024).

58. K. Novović, B. Jovčić, Colistin Resistance in Acinetobacter baumannii: Molecular Mechanisms and Epidemiology. *Antibiotics (Basel)* **12**, 516 (2023).

59. L. Lin, *et al.*, Inhibition of LpxC protects mice from resistant Acinetobacter baumannii by modulating inflammation and enhancing phagocytosis. *mBio* **3** (2012).

60. G. E, H. W, H.-B. J, I. RR, Acinetobacter baumannii: Envelope Determinants That Control Drug Resistance, Virulence, and Surface Variability. *Annual review of microbiology* **73**, 481–506 (2019).

61. S. Gerson, *et al.*, Investigation of Novel pmrB and eptA Mutations in Isogenic Acinetobacter baumannii Isolates Associated with Colistin Resistance and Increased

Virulence In Vivo. *Antimicrobial Agents and Chemotherapy* **63**, 10.1128/aac.01586-18 (2019).

62. C. Cooper, *et al.*, H-NS is a bacterial transposon capture protein. *Nat Commun* **15**, 7137 (2024).

63. C. J. Dorman, H-NS, the genome sentinel. *Nat Rev Microbiol* **5**, 157–161 (2007).

64. A. O. Olaitan, S. Morand, J.-M. Rolain, Mechanisms of polymyxin resistance: acquired and intrinsic resistance in bacteria. *Frontiers in microbiology* **5**, 643 (2014).

65. E. S. Snitkin, *et al.*, Genomic insights into the fate of colistin resistance and Acinetobacter baumannii during patient treatment. *Genome Res.* **23**, 1155–1162 (2013).

66. S. Y. Ko, *et al.*, PmrAB controls virulence-associated traits and outer membrane vesicle biogenesis in *Acinetobacter baumannii*. *Microbial Pathogenesis* **185**, 106434 (2023).

67. S. Subashchandrabose, *et al.*, Acinetobacter baumannii Genes Required for Bacterial Survival during Bloodstream Infection. *mSphere* **1**, e00013-15 (2015).

68. N. Wang, E. A. Ozer, M. J. Mandel, A. R. Hauser, Genome-wide identification of Acinetobacter baumannii genes necessary for persistence in the lung. *mBio* **5**, e01163-14 (2014).

69. P. K. Jangir, L. Ogunlana, R. C. MacLean, Evolutionary constraints on the acquisition of antimicrobial peptide resistance in bacterial pathogens. *Trends in Microbiology* **29**, 1058–1061 (2021).

70. V. C. Thai, K. A. Stubbs, M. Sarkar-Tyson, C. M. Kahler, Phosphoethanolamine Transferases as Drug Discovery Targets for Therapeutic Treatment of Multi-Drug Resistant Pathogenic Gram-Negative Bacteria. *Antibiotics (Basel)* **12**, 1382 (2023).

71. J. C. Henderson, *et al.*, The Power of Asymmetry: Architecture and Assembly of the Gram-Negative Outer Membrane Lipid Bilayer. *Annual Review of Microbiology* **70**, 255–278 (2016).

72. C. D. M. Wijers, *et al.*, Identification of Two Variants of Acinetobacter baumannii Strain ATCC 17978 with Distinct Genotypes and Phenotypes. *Infection and Immunity* **89** (2021).

73. E. Geisinger, R. R. Isberg, Antibiotic Modulation of Capsular Exopolysaccharide and Virulence in Acinetobacter baumannii. *PLOS Pathogens* **11**, e1004691 (2015).

74. H. L. Andrews, J. P. Vogel, R. R. Isberg, Identification of Linked Legionella pneumophila Genes Essential for Intracellular Growth and Evasion of the Endocytic Pathway. *Infection and Immunity* **66**, 950–958 (1998).

75. J. H. Moffatt, *et al.*, Colistin Resistance in Acinetobacter baumannii Is Mediated by Complete Loss of Lipopolysaccharide Production. *Antimicrobial Agents and Chemotherapy* **54**, 4971–4977 (2010).

76. E. Wang, *et al.*, Pathogenesis of Pneumococcal Pneumonia in Cyclophosphamide-Induced Leukopenia in Mice. *Infection and Immunity* **70**, 4226–4238 (2002).

77. T. B. Nielsen, J. Yan, B. Luna, B. Spellberg, Murine Oropharyngeal Aspiration Model of Ventilator-associated and Hospital-acquired Bacterial Pneumonia. *J Vis Exp* 57672 (2018). https://doi.org/10.3791/57672.

78. Y.-W. Lin, *et al.*, Elucidating the Pharmacokinetics/Pharmacodynamics of Aerosolized Colistin against Multidrug-Resistant Acinetobacter baumannii and Klebsiella pneumoniae in a Mouse Lung Infection Model. *Antimicrobial agents and chemotherapy* **62** (2018).

79. T. Sharafi, A. Ardebili. Plastic binding feature of polymyxins: the effect on MIC susceptibility measurements. *IDR* **12**, 2649–2653 (2019).

80. J. E. Choby, *et al.*, Copy number flexibility facilitates heteroresistance to increasing antibiotic pressure and threatens the beta-lactam pipeline. *Nat Commun* **16**, 5721 (2025).

81. D. E. Deatherage, J. E. Barrick, "Identification of Mutations in Laboratory-Evolved Microbes from Next-Generation Sequencing Data Using breseq" in *Engineering and Analyzing Multicellular Systems: Methods and Protocols*, L. Sun, W. Shou, Eds. (Springer, 2014), pp. 165–188.

82. S. Koren, *et al.*, Canu: scalable and accurate long-read assembly via adaptive k-mer weighting and repeat separation. *Genome Res.* **27**, 722–736 (2017).

83. M. J. Powers, C. M. Herrera, A. T. Tucker, B. W. Davies, M. S. Trent, "Isolation of Lipid Cell Envelope Components from Acinetobacter baumannii" in *Acinetobacter Baumannii: Methods and Protocols*, I. Biswas, P. N. Rather, Eds. (Springer, 2019), pp. 233–252.

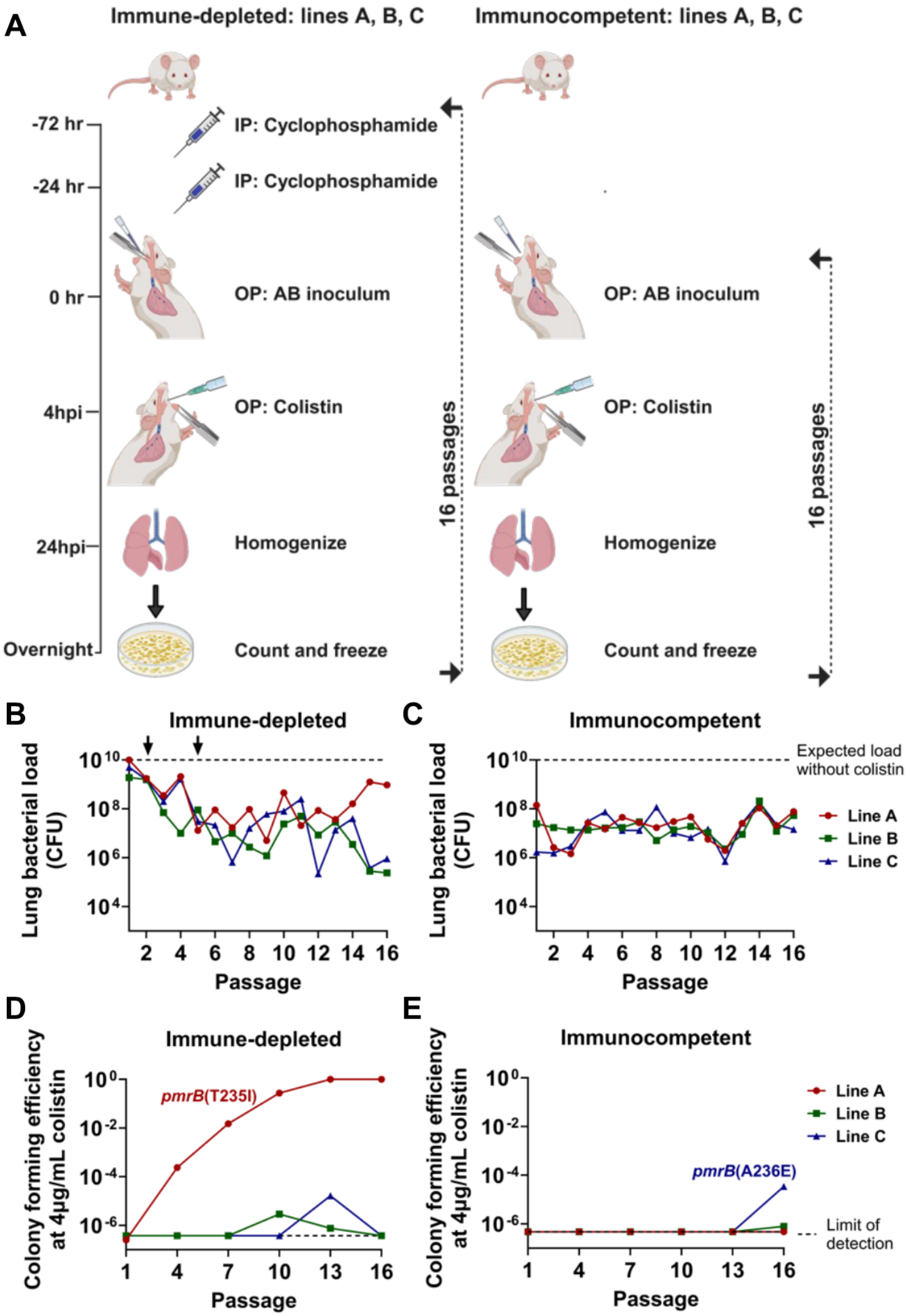
A
Immune-depleted: lines A, B, C
Immunocompetent: lines A, B, C
-72 hr
IP: Cyclophosphamide
-24 hr
IP: Cyclophosphamide
0 hr
OP: AB inoculum
4hpi
OP: Colistin
24hpi
Homogenize
Overnight
Count and freeze
16 passages
B
Immune-depleted
Lung bacterial load (CFU)
Passage
C
Immunocompetent
Expected load without colistin
Line A
Line B
Line C
D
Immune-depleted
Colony forming efficiency at 4µg/mL colistin
pmrB(T235I)
E
Immunocompetent
pmrB(A236E)
Limit of detection

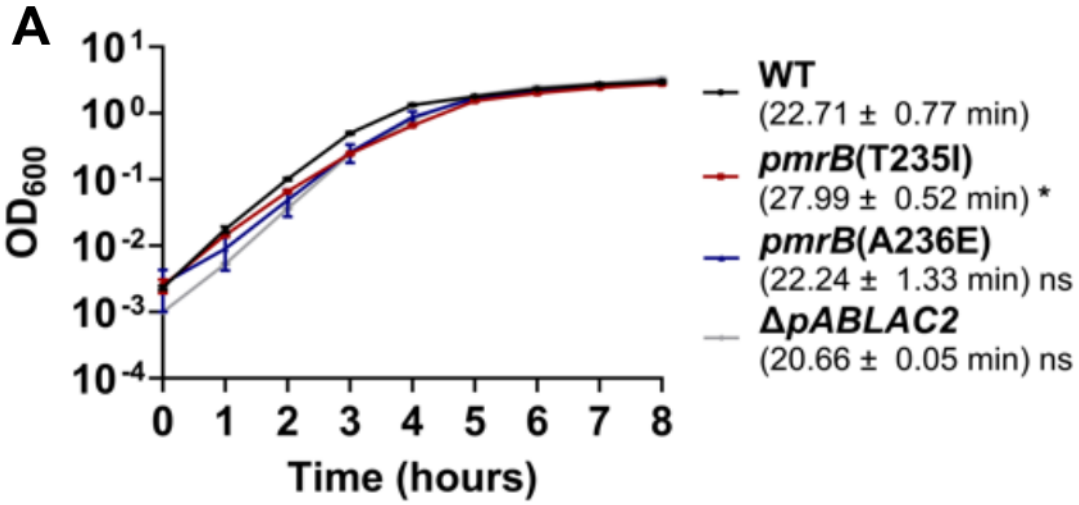
A
OD600
Time (hours)
WT
(22.71 ± 0.77 min)
pmrB(T235I)
(27.99 ± 0.52 min) *
pmrB(A236E)
(22.24 ± 1.33 min) ns
ΔpABLAC2
(20.66 ± 0.05 min) ns

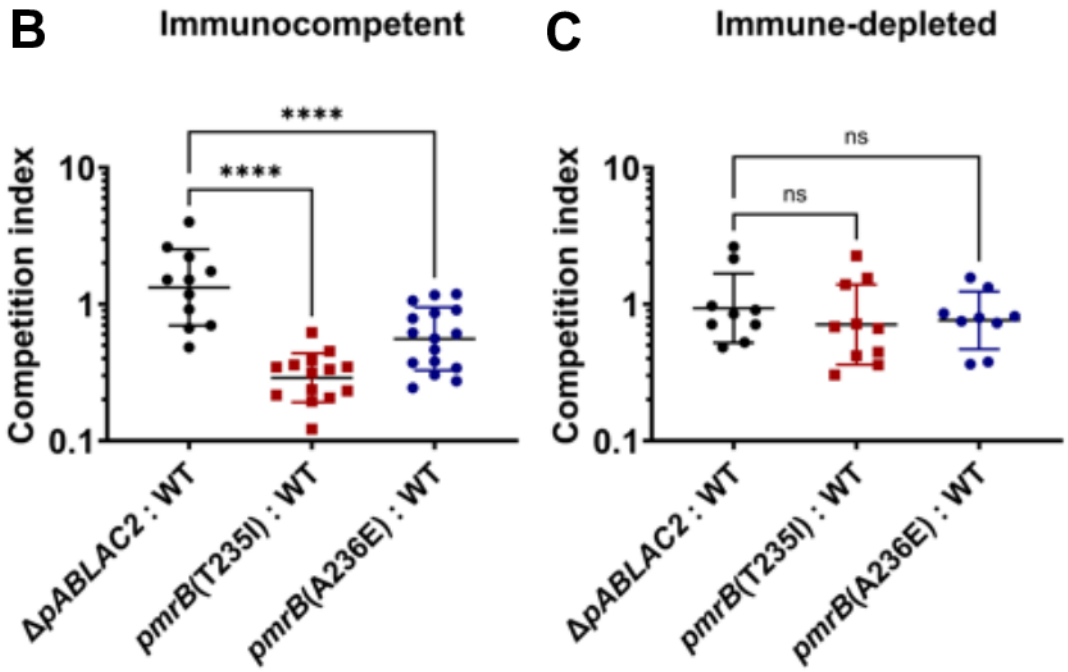
B
Immunocompetent
C
Immune-depleted
Competition index
****
****
ns
ns
ΔpABLAC2 : WT
pmrB(T235I) : WT
pmrB(A236E) : WT

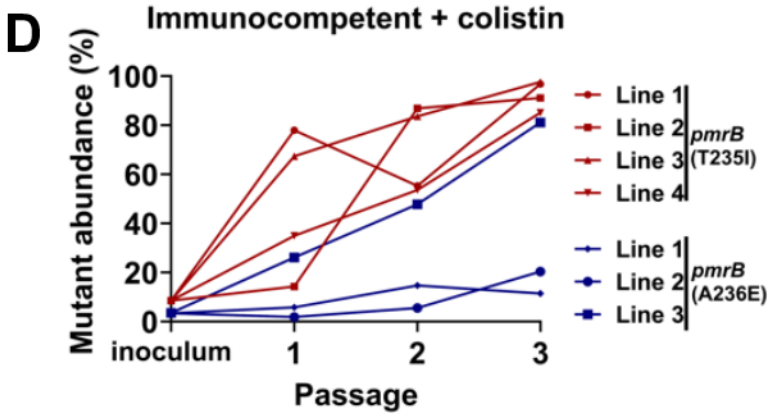
D
Immunocompetent + colistin
Mutant abundance (%)
Passage
inoculum
Line 1
Line 2
Line 3
Line 4
pmrB (T235I)
Line 1
Line 2
Line 3
pmrB (A236E)

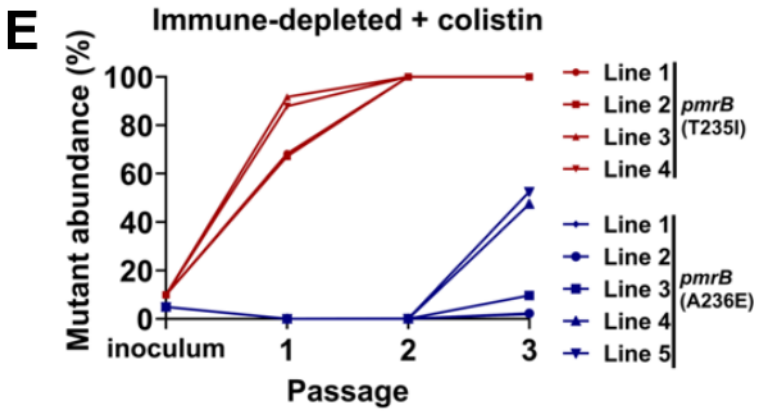
E
Immune-depleted + colistin
Mutant abundance (%)
Passage
inoculum
Line 1
Line 2
Line 3
Line 4
pmrB (T235I)
Line 1
Line 2
Line 3
Line 4
Line 5
pmrB (A236E)

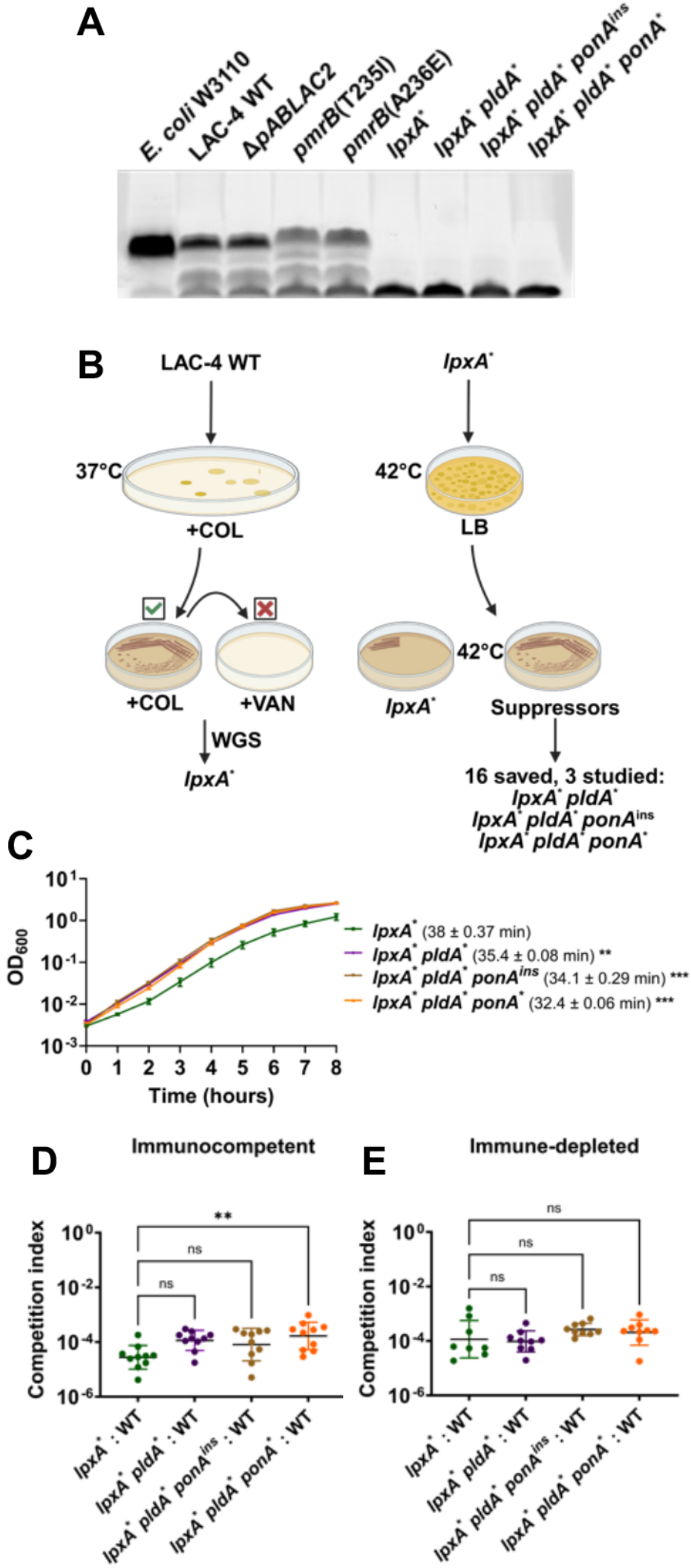
A
E. coli W3110
LAC-4 WT
ΔpABLAC2
pmrB(T235I)
pmrB(A236E)
lpxA*
lpxA* pldA*
lpxA* pldA* ponA^ins
lpxA* pldA* ponA*
B
LAC-4 WT
lpxA*
37°C
+COL
42°C
LB
+COL
+VAN
42°C
lpxA*
Suppressors
WGS
lpxA*
16 saved, 3 studied:
lpxA* pldA*
lpxA* pldA* ponA^ins
lpxA* pldA* ponA*
C
OD600
Time (hours)
lpxA* (38 ± 0.37 min)
lpxA* pldA* (35.4 ± 0.08 min) **
lpxA* pldA* ponA^ins (34.1 ± 0.29 min) ***
lpxA* pldA* ponA* (32.4 ± 0.06 min) ***
D
Immunocompetent
Competition index
ns
ns
**
lpxA* : WT
lpxA* pldA* : WT
lpxA* pldA* ponA^ins : WT
lpxA* pldA* ponA* : WT
E
Immune-depleted
Competition index
ns
ns
ns
lpxA* : WT
lpxA* pldA* : WT
lpxA* pldA* ponA^ins : WT
lpxA* pldA* ponA* : WT

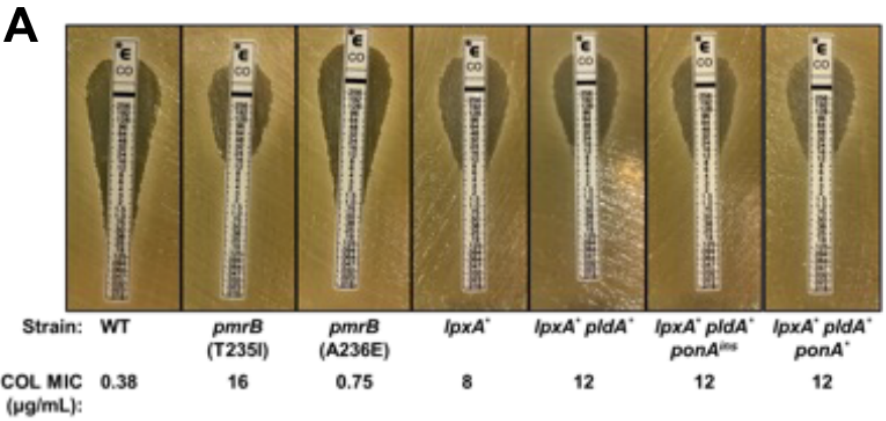
A
Strain: WT
pmrB (T235I)
pmrB (A236E)
lpxA*
lpxA* pldA*
lpxA* pldA* ponA^ins
lpxA* pldA* ponA*
COL MIC (µg/mL): 0.38 16 0.75 8 12 12 12

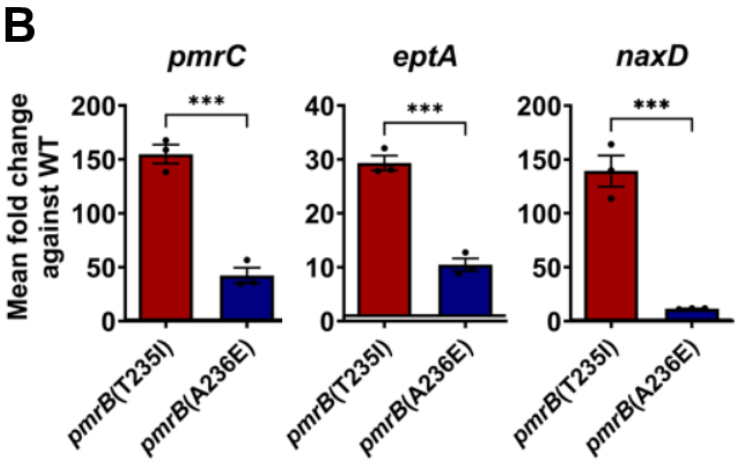
B
pmrC
eptA
naxD
Mean fold change against WT
***
pmrB(T235I)
pmrB(A236E)

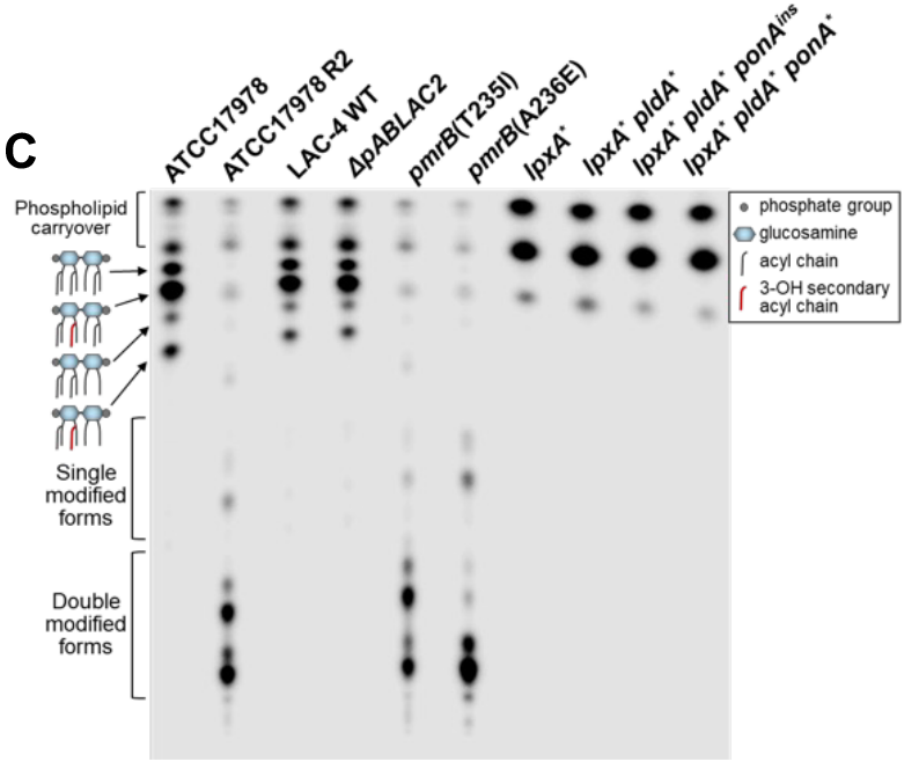
C
ATCC17978
ATCC17978 R2
LAC-4 WT
ΔpABLAC2
pmrB(T235I)
pmrB(A236E)
lpxA*
lpxA* pldA*
lpxA* pldA* ponA^ins
lpxA* pldA* ponA*
Phospholipid carryover
Single modified forms
Double modified forms
phosphate group
glucosamine
acyl chain
3-OH secondary acyl chain

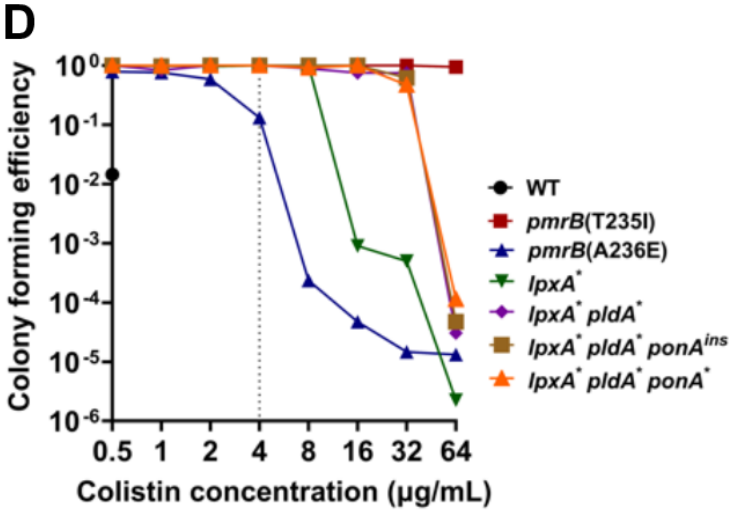
D
Colony forming efficiency
Colistin concentration (µg/mL)
WT
pmrB(T235I)
pmrB(A236E)
lpxA*
lpxA* pldA*
lpxA* pldA* ponA^ins
lpxA* pldA* ponA*

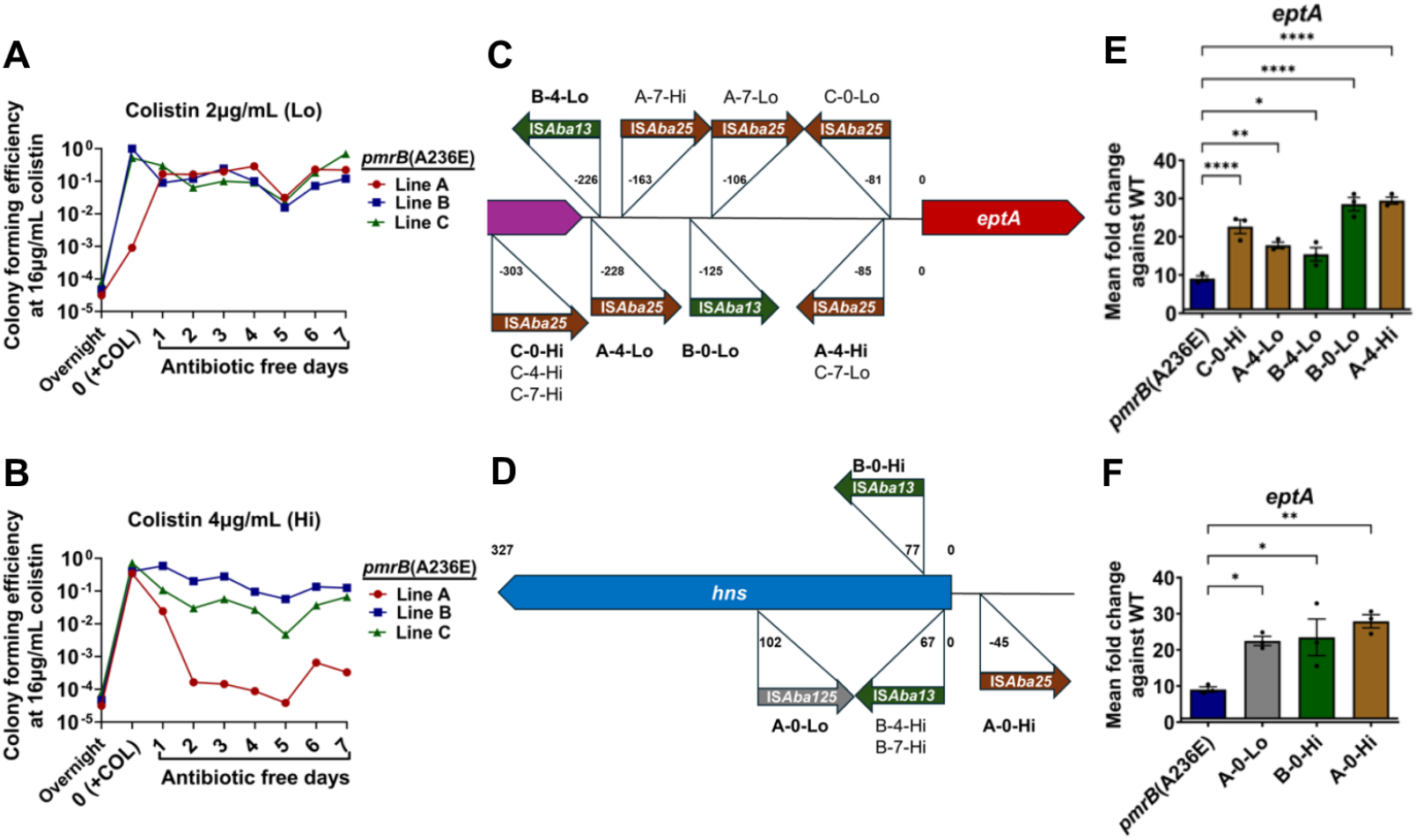
A
Colistin 2μg/mL (Lo)
Colony forming efficiency at 16μg/mL colistin
pmrB(A236E)
Line A
Line B
Line C
Overnight
0 (+COL)
Antibiotic free days
B
Colistin 4μg/mL (Hi)
C
B-4-Lo
A-7-Hi
A-7-Lo
C-0-Lo
ISAba13
ISAba25
eptA
C-0-Hi
C-4-Hi
C-7-Hi
A-4-Lo
B-0-Lo
A-4-Hi
C-7-Lo
D
B-0-Hi
hns
ISAba125
A-0-Lo
B-4-Hi
B-7-Hi
A-0-Hi
E
Mean fold change against WT
F

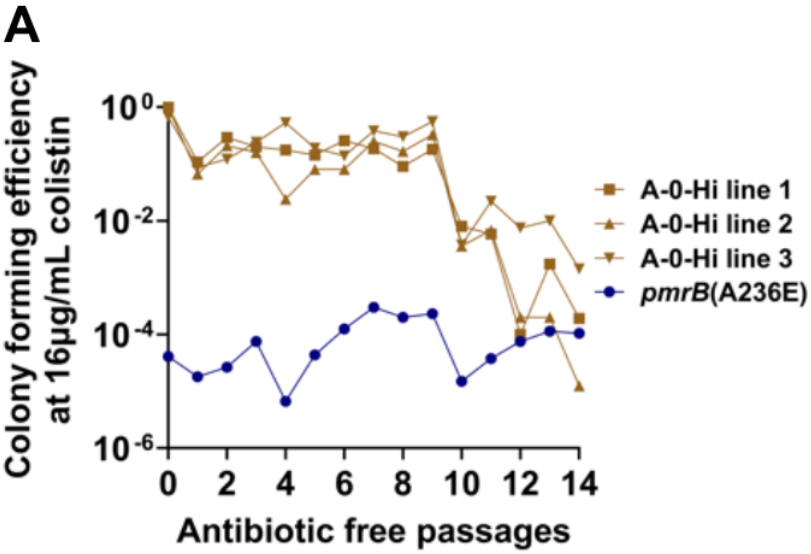

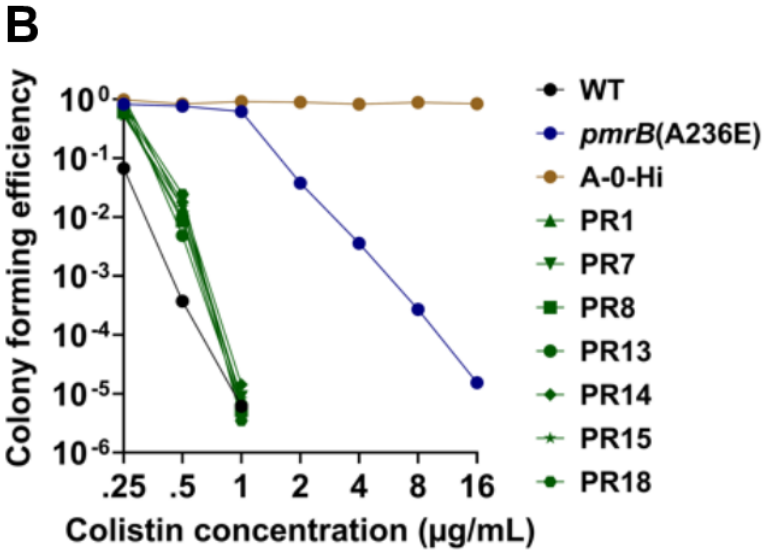

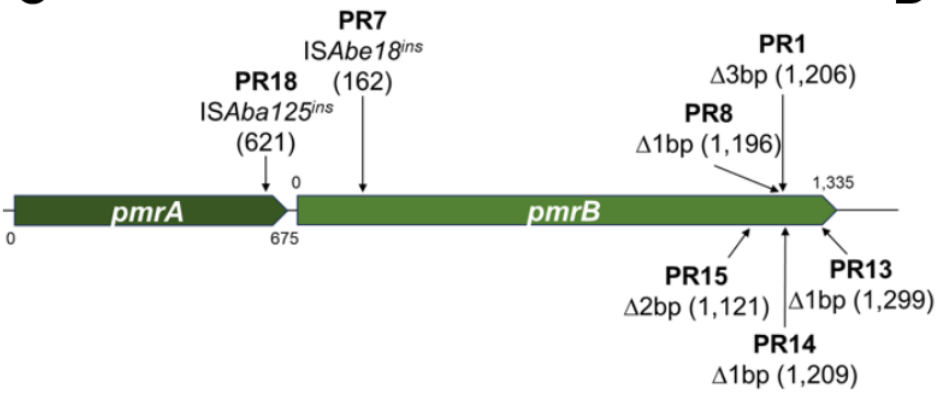

D

Strain:	Doubling time (minutes):
A-0-Hi	19.73 ± 0.16
PR1	19.38 ± 0.14 (ns)
PR7	19.16 ± 0.18 (ns)
PR8	20.19 ± 0.24 (ns)
PR13	19.08 ± 0.23 (ns)
PR14	19.02 ± 0.14 (ns)
PR15	18.77 ± 0.27 (*)
PR18	20.04 ± 0.18 (ns)
WT	17.32 ± 0.04 (****)

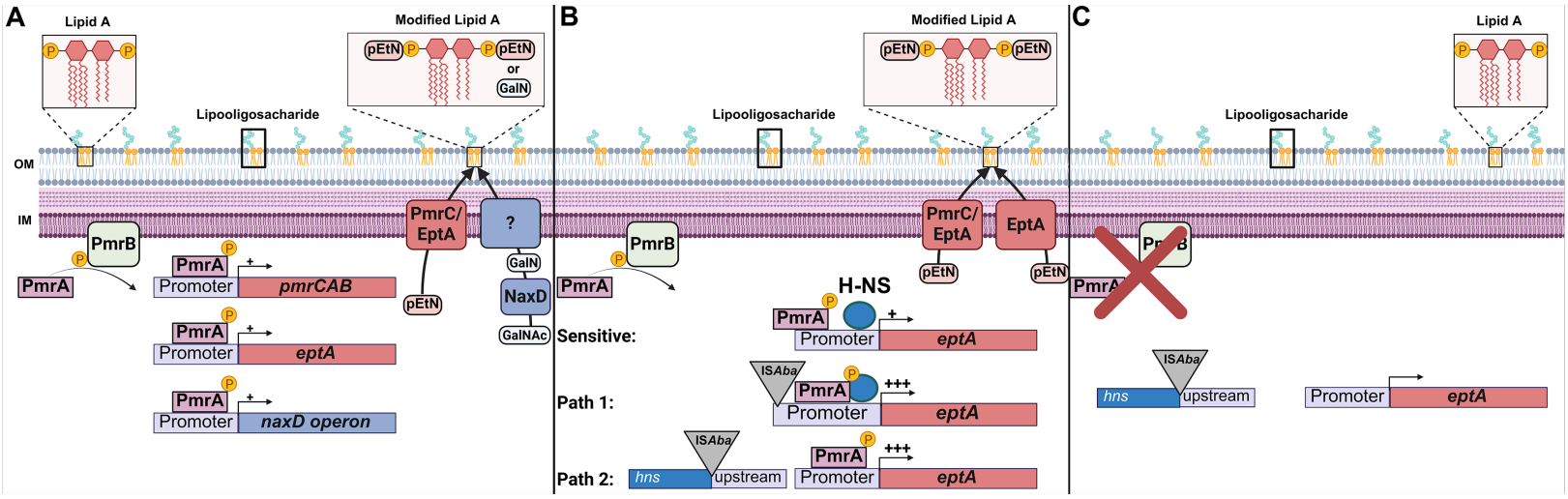
A
Lipid A
Modified Lipid A
pEtN
or
GalN
Lipooligosacharide
OM
IM
PmrB
PmrA
Promoter
pmrCAB
eptA
naxD operon
PmrC/
EptA
?
NaxD
GalNAc
B
H-NS
Sensitive:
Path 1:
Path 2:
ISAba
hns
upstream
EptA
C